JGR Biogeosciences

RESEARCH ARTICLE
10.1029/2021JG006657

Key Points:

- The water column nutrient level controlled the horizontal distribution of Noelaerhabdaceae coccolithophore cell abundance
- Noelaerhabdaceae coccolithophores contributed to <18% of seawater particulate inorganic carbon in the South China Sea
- The degree of Emiliania huxleyi coccolith calcification was insensitive to carbonate chemistry for the investigated waters

Supporting Information:

Supporting Information may be found in the online version of this article.

Correspondence to:

X. Jin and C. Liu,
386jinxiaobo@tongji.edu.cn;
liucl@tongji.edu.cn

Citation:

Jin, X., Liu, C., Xu, J., & Guo, X. (2022). Coccolithophore abundance, degree of calcification, and their contribution to particulate inorganic carbon in the South China Sea. *Journal of Geophysical Research: Biogeosciences*, *127*, e2021JG006657. https://doi.org/10.1029/2021JG006657

Received 4 OCT 2021
Accepted 14 MAR 2022

Author Contributions:

Conceptualization: Xiaobo Jin, Chuanlian Liu
Funding acquisition: Xiaobo Jin, Chuanlian Liu
Investigation: Xiaobo Jin, Xianghui Guo
Methodology: Xiaobo Jin, Juan Xu, Xianghui Guo
Supervision: Chuanlian Liu
Writing – original draft: Xiaobo Jin
Writing – review & editing: Xiaobo Jin, Chuanlian Liu

Coccolithophore Abundance, Degree of Calcification, and Their Contribution to Particulate Inorganic Carbon in the South China Sea

Xiaobo Jin[1], Chuanlian Liu[1], Juan Xu[1], and Xianghui Guo[2]

[1]State Key Laboratory of Marine Geology, Tongji University, Shanghai, China, [2]State Key Laboratory of Marine Environmental Science, Xiamen University, Xiamen, China

Abstract Particulate inorganic carbon (PIC) production and export to deep ocean are important processes in water column carbonate cycling. Biochemistry investigations have shown that the seawater PIC in eutrophic high-latitude waters is contributed by marine calcifying algae coccolithophores which are constituted by the nearly monospecies *Emiliania huxleyi*. This allows the seawater PIC to be predicted in these high-fertility regions based on satellite remote sensing. However, in waters with low surface PIC productivity, which still account for 70% of global ocean areas, the subsurface PIC maximum may not be well disclosed by satellite. Here, with a biochemistry cruise, we investigated the seawater coccolithophore cell and coccolith abundances, degree of *E. huxleyi* coccolith calcification, and PIC concentration in the deep chlorophyll maximum layers in the South China Sea, with the aim to improve our understanding of PIC production in these low productivity regions. Our results demonstrate the control of nutrient levels in the water column on the geographical (horizontal) distribution of Noelaerhabdaceae coccolithophores (*E. huxleyi* and *Gephyrocapsa oceanica*) in the investigated area, as well as an insensitive response of the calcification degree of *E. huxleyi* coccolith to carbonate chemistry. Although Noelaerhabdaceae coccoliths were the major components of deep-sea sediment carbonate, they on average contributed to <18% of suspended PIC for the investigated seawater, indicating multiple sources of highly variable suspended PIC in the subsurface oligotrophic water. The production of Noelaerhabdaceae coccoliths greatly depends on local environments, which highlights the importance of field investigations in low-fertility areas for global PIC productivity evaluation.

Plain Language Summary Marine carbonate calcium production is an important process in modulating global ocean alkalinity which impacts oceanic carbon dioxide release and absorption. Calcifying marine algae, coccolithophores, are important calcium carbonate producers. Hence, understanding their contribution to seawater suspended particulate calcium carbonate is important for understanding the global carbon cycle. Coccolithophore production can be detected by satellite in the high-latitude and high-fertility oceans; however, this method may be challenging at estimating coccolithophore production in low-fertility waters. Here, we investigated the coccolithophore abundance and the particulate calcium carbonate concentration of seawater in the South China Sea, a low fertility region. Our results show that the euphotic nutrient level and the seawater nitrogen and silicon nutrient distributions control coccolithophore production and their contribution to seawater carbonate particles.

1. Introduction

Coccolithophores are a group of marine calcifying algae which produce calcite scales, namely, coccoliths. The production of coccoliths reduces sea surface ocean alkalinity, and dissolved inorganic carbon and elevates seawater pCO_2. It is acknowledged that coccolith-based calcite contributes to nearly half of calcium carbonate ($CaCO_3$) export and storage in deep ocean and marine sediments (Broecker & Clark, 2009; Young & Ziveri, 2000). For the geological past, changes in marine coccolith calcite production impacted deep carbonate cycling and carbonate-counter pump, which potentially contributed to local seawater CO_2 outgassing during the glacial-interglacial stages (Balestrieri et al., 2021; Duchamp-Alphonse et al., 2018; Saavedra-Pellitero et al., 2017). For modern oceans, the blooming of coccolithophores can change surface alkalinity and impact CO_2 exchanges between the ocean and atmosphere (Balch et al., 2005, 2016). Therefore, coccolithophores are an important component in global biogeochemical cycles and are expected to play a significant role in global seawater CO_2 buffer and in oceanic sink for anthropogenic CO_2. Knowledge of the global coccolith-based calcite distribution

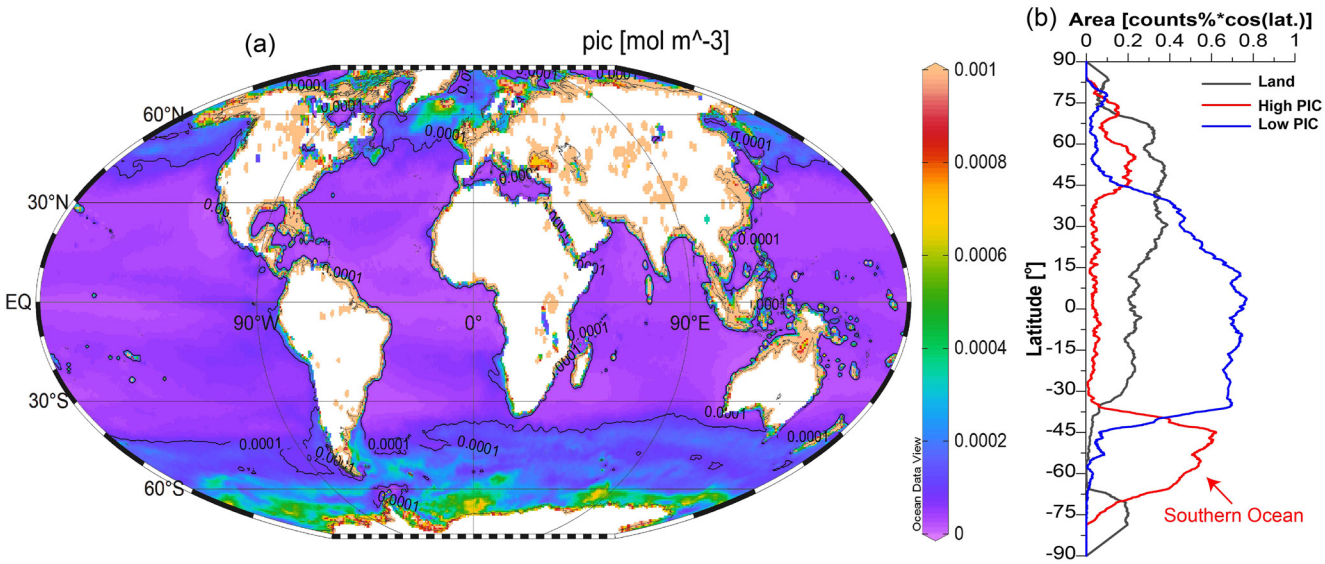

Figure 1. (a) Satellite remote sensing-based global surface ocean PIC concentration (mol m^{-3}) (MODIS-Aqua entire mission composited data, up to January 2021, https://oceancolor.gsfc.nasa.gov/l3/). (b) Meridional distribution of the global relative ocean and land areas. The red and blue curves indicate the oceans with high and low PIC concentrations, respectively, in terms of a threshold value of 0.1 mmol C m^{-3}. The low PIC regions account for approximately 70% of global ocean areas. Map (a) was drawn using Ocean Data View (ODV, Schlitzer, 2021).

as well as their contributions to seawater particulate inorganic carbon (PIC) can help us to understand their roles in these aspects.

An effective way to estimate modern surface ocean PIC concentrations is using satellite-based remote sensing reflectance (Balch, 2018; Balch et al., 2005). Together with field investigations, it is found that approximately 1/4 of the global surface suspended PIC standing stock is found in the Southern Ocean (Figure 1a), which only covers 16% of the global ocean area (Balch et al., 2005). The suspended PIC in the Southern Ocean called the "Great Calcite Belt" results from the coccolithophore *Emiliania huxleyi* blooming that produces massive coccolith calcite in surface waters (Balch et al., 2011, 2016). Hence, the importance of coccolithophores in biogeochemical cycles of these eutrophic high-latitude waters has been shown. However, few studies have addressed the PIC standing stock and the potential contributions of coccolithophores in oligotrophic oceans, for example, in tropical and subtropical waters, where the satellite-based surface PIC concentration is extremely low (Figure 1a; Balch et al., 2005). In these areas, the layers of deep chlorophyll maximum (DCM) are usually well developed, and the reflectance or backscattering of coccolith-based PIC in a deeper layer of the euphotic zone may not be detected by satellites. Balch et al. (2018) indicated that when the surface concentration of PIC was extremely low (<0.1 mmol PIC m^{-3}) in low fertility oceans, the subsurface PIC maximum could be developed in the euphotic zones; however, the highly variable subsurface PIC concentration might not be well reflected by their surface concentration. Since the oligotrophic and low productivity regions still represent the majority of global ocean areas (approximately 70%, Figure 1b), coccolith calcite production in the subsurface layer of these areas may still contribute a considerable amount to global PIC production, which could be important for ocean carbon cycles.

To evaluate the potential importance of coccolithophores in ocean biochemistry cycles in oligotrophic oceans, we investigated the seawater PIC, coccolithophore and detached coccolith concentrations, and the degree of coccolith calcification in the subsurface DCM during an oligotrophic season in the South China Sea (SCS). A previous investigation in the SCS has shown that the highest coccolithophore cell and coccolith concentrations were found within the DCM layers of water column (Jin et al., 2016), and the biochemistry information (e.g., biomass) in the DCM of these low fertility areas should be representative of those of the integrated euphotic water column (Balch et al., 2018).

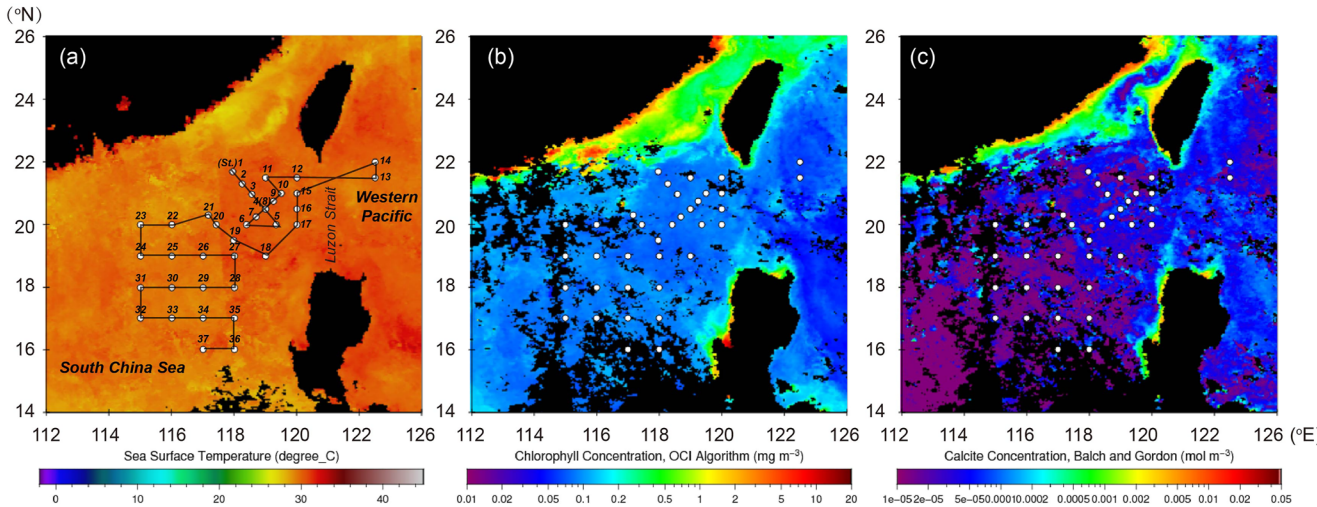

Figure 2. Map of the sampling stations of cruise NORC2018-05 in the South China Sea, superimposed on satellite-based sea surface temperature (a), chlorophyll concentration (b), and calcite concentration (Balch et al., 2005) (c) in June 2018. Stations (St.) 1 to 37 and the solid line in (a) also indicates the trajectory of the cruise. All satellite-based data were derived at https://oceancolor.gsfc.nasa.gov/.

2. Cruise and Sampling

The field investigation was conducted on board the research vessel "TAN KAH KEE (JiaGeng)" during cruise NORC2018-05 from June to July 2018. The cruise trajectory passed through 35 stations in the SCS and 2 stations in the Western Pacific (Figure 2a; Table S1 in Supporting Information S1). The investigated area was characterized by an oligotrophic ocean during the summer season, with high sea surface temperature (>28°C), and low surface chlorophyll and PIC concentrations (<0.1 mmol C m^{-3}; Figures 2a–2c). Along the cruise trajectory, the investigated area can be divided into four regions: the northeastern SCS (NE-SCS), the Western Pacific (WP), the northern SCS (N-SCS), and the basin SCS (B-SCS) (Figure 3a). The *in situ* measured seawater physical and chemical parameters (Figures 3b–3f) by conductivity-temperature-depth (CTD) showed that the water column was strongly stratified, and a DCM was well developed at all stations. Revealed by the photosynthetically active radiation (PAR) sensor, the euphotic depth (1% of surface irradiance) was approximately 80–100 m at the SCS stations, and 125 m at the WP stations, and the depth of 10% of surface irradiance was at approximately 50–70 m of the water column depth for the investigated waters (Figure 3f). Hence, the DCM was generally in line with the 10% surface irradiance layer in the water column. Water samples were collected using a CTD rosette sampler in the DCM layer of each station.

3. Methods

3.1. Coccolithophore and Detached Coccolith Concentrations

Two liters of water sample at each station was gently filtered through 0.8 μm pore-size and 25 mm diameter polycarbonate membranes using a vacuum pump. The membranes were rinsed with deionized water and dried on a hot plate. A small piece of a membrane sample was cut and fixed within a slide and cover slip using Norland Optical Adhesive (No. 74). Coccolithophore cells and detached coccoliths were counted in the slides using a polarized light microscope (Zeiss Axio) at ×1,000 magnification. The cell or coccolith concentration (CC, cells or coccolith mL^{-1}) can be calculated:

$$CC = A * N_C/(S * V) \quad (1)$$

where A is the area of filtration (415.47 mm^2), N_C is the total number of cells or coccoliths counted, S is the total area of fields of view (FOVs, area per FOV is 0.0394 mm^2) inspected, and V is the filtered seawater volume (2,000 mL). Coccolithophore cells were counted in at least 50 FOVs, suggesting that at least 9.48 mL of seawater was analyzed. The detection limit of a cell at the 95% probability level can be calculated following a Poisson distribution (Bollmann et al., 2002):

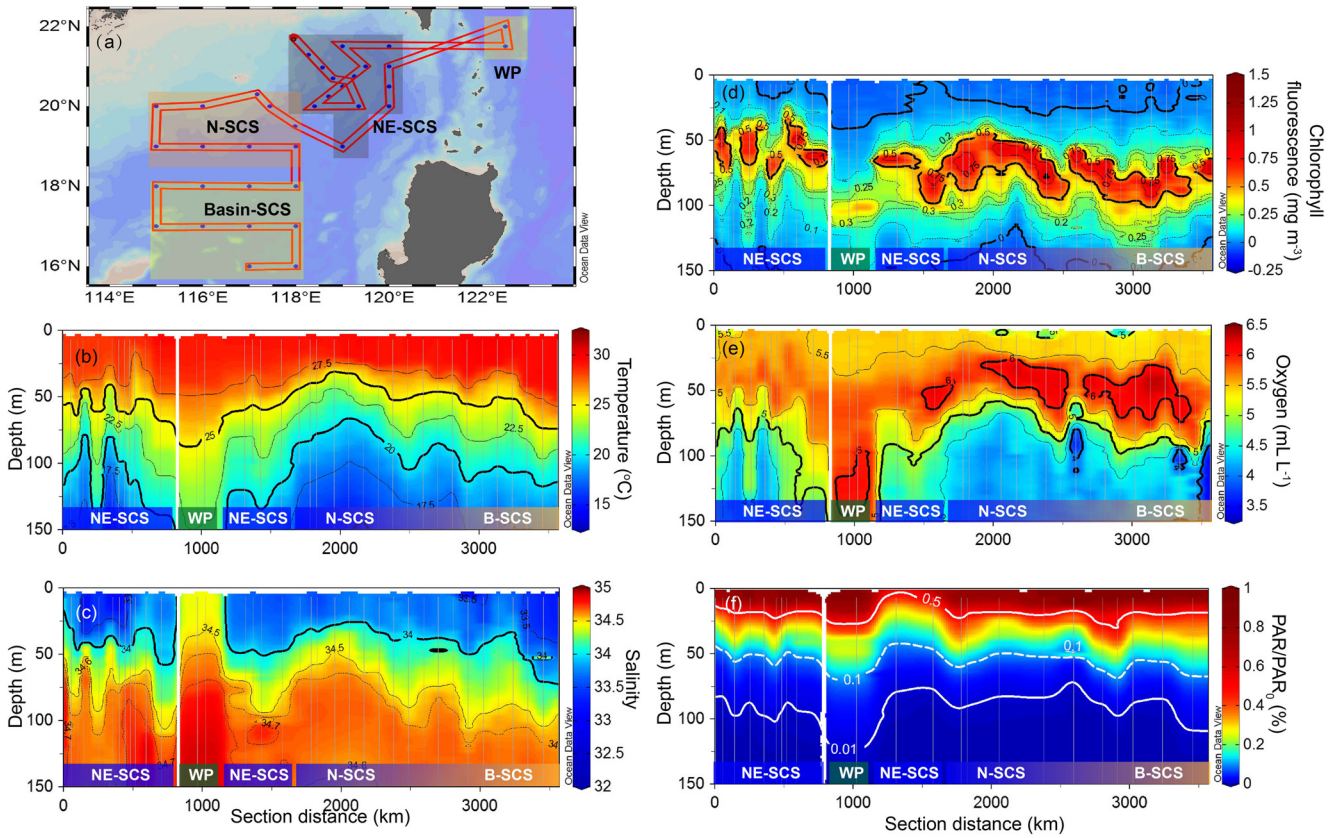

Figure 3. (a) The trajectory, four regions can be divided: the northeastern SCS (NE-SCS), the Western Pacific (WP), and the northern to basin SCS (N-SCS to B-SCS). (Note that the position of Station 4 was slightly moved to easily plot the sections using ODV.) Panels (b) to (f) show the CTD-based seawater temperature, salinity, chlorophyll fluorescence, oxygen concentration, and relative photosynthetically active radiation (PAR) to surface (PAR/PAR_0) along the trajectory.

$$\chi = x * y > -\ln(0.05) \tag{2}$$

where x is the detection limit (cells mL^{-1}) and y is the amount of seawater sample analyzed. The cell counting strategy gives a detection limit of at least 0.32 cell mL^{-1}. Coccolithophore cells were counted in several groups. First, *E. huxleyi*, *Gephyrocapsa oceanica*, *Florisphaera profunda*, and *Algirosphaera robusta* cells were counted. These species are the four most commonly seen in the modern SCS (Jin et al., 2016; Sun et al., 2011). Second, we counted the *Calcidiscus* and *Helicosphaera* cells. Their cells/coccospheres potentially contribute to a large amount of PIC in seawater due to their relatively higher calcite content per coccolith (Young & Ziveri, 2000; Ziveri et al., 2007). Third, we counted the upper euphotic zone (UPZ or UEZ) coccolithophores which include the coccospheres of *Umbellosphaera* spp., *Discosphaera* spp., and *Rhabdosphaera* spp. (Jin et al., 2016). Finally, we counted the "rare species" group noted by Poulton et al. (2017). A genus or species that belongs to the "rare" group may account for a small portion of the total cell abundance, however, they are especially diverse (Poulton et al., 2017). The "rare species" group we counted includes the genera *Calciosolenia*, *Michaelsarsia*, *Syracosphaera*, *Oolithotus*, and *Umbilicosphaera*. Detached coccoliths (or nannoliths for *F. profunda*) were counted for more than 250 individuals or at least in 10 FOVs. Here, only *E. huxleyi*, *G. oceanica*, and *F. profunda* were counted.

3.2. Seawater PIC Concentration

Another three liters of water sample at each station was filtered through 0.8 μm pore-size and 47 mm diameter polycarbonate membranes, and the membranes were rinsed with deionized water and dried. The principle of seawater PIC analysis followed Poulton et al. (2006) and Daniels et al. (2012). A membrane sample was put into a 15 mL centrifuge tube, and reacted with 10 mL of 2% nitric acid for 2 h. Then, 2 mL of the suspension was

micropipetted and diluted into 4 g (approximately 4 mL) in another 15 mL centrifuge tube. $[Ca^{2+}]$ (unit in parts per million mass, ppm) of the solution was analyzed using inductively coupled plasma–mass spectrometry (ICP–MS, Agilent 7900). The measured $[Ca^{2+}]$ can originate from (a) calcium release from $CaCO_3$ dissolution and (b) residual seawater on filters (Figure S1 in Supporting Information S1). To remove the influence of the seawater residual, $[Ca^{2+}]$ was corrected by the measured $[K^+]$ in the solution:

$$\left[Ca^{2+}\right]_{\text{corrected}} = \left[Ca^{2+}\right] - \left[K^+\right] * \left(\left[Ca^{2+}\right]/\left[K^+\right]\right)_{\text{seawater}} \quad (3)$$

where $([Ca^{2+}]/[K^+])_{\text{seawater}}$ is the mass ratio of $[Ca^{2+}]$ and $[K^+]$ of seawater. $[K^+]$ can be a proper anchoring for $[Ca^{2+}]$, because both the ion radius and seawater mass fractions of $[K^+]$ and $[Ca^{2+}]$ are comparable. Here, the value of $([Ca^{2+}]/[K^+])_{\text{seawater}}$ used here is 412/399 (Dickson & Goyet, 1994). The seawater PIC concentration (pg $CaCO_3$ mL^{-1}) can then be calculated as:

$$\text{PIC} = \left[Ca^{2+}\right]_{\text{corrected}} * w * f * \left(\frac{100}{40}\right)/v \quad (4)$$

where w is the weight of the solution measured (4 g), f is a dilution factor (here, $f = 5$), 100/40 is the molar mass ratio of $CaCO_3$ to calcium, and v is the filtered seawater volume (3,000 mL). Measurements for triplicate sampling at station (St.) 30 was conducted, showing that the relative standard deviation for $[Ca^{2+}]_{\text{corrected}}$ was 4.96%.

3.3. Quantifying Coccolith-Based Calcite From Key Species and Genera

Here, we estimated the seawater coccolith calcite content from *E. huxleyi*, *G. oceanica*, *F. profunda*, *Calcidiscus* spp., and *Helicosphaera* spp. *E. huxleyi*, *G. oceanica*, and *F. profunda* represent the major components of the coccolith assemblages as seen in sediment trap materials (Chen et al., 2007; Jin, Liu, Zhao, et al., 2019; Priyadarshani et al., 2019) and surface sediments (Cheng & Wang, 1997; Fernando et al., 2007) in the SCS. *Calcidiscus* and *Helicosphaera* coccoliths were also found to be one of the dominant coccolith calcite contributors in the deep water column in high latitude oceans (Ziveri et al., 2007). Therefore, the production and downward transport of coccolith calcite of these key species and genera could be important for water column carbonate cycling in the SCS.

The calcite content of a cell was resolved by multiplying the number of coccoliths per cell by the average coccolith calcite mass of a specific species. The number of coccoliths of a cell or coccosphere for *E. huxleyi* (24 coccoliths per cell), *G. oceanica* (23 coccoliths per cell), *F. profunda* (62 nannoliths per cell), *Calcidiscus* spp. (21 coccoliths per cell), and *Helicosphaera* spp. (21 coccoliths per cell) was obtained from Boeckel and Baumann (2008) and Yang and Wei (2003). The average coccolith mass was determined by coccolith optical properties under light microscopy following the principle that coccolith thickness was proportional to its lightness (Beaufort, 2005). Coccoliths were photographed as black–white images using a digital camera (Zeiss AxioCam MRc 5) under circular polarized light (Bollmann, 2014; Fuertes et al., 2014) at ×1,250 magnification (resolution = 0.088 μm $pixel^{-1}$). The gray level, area, and length of a coccolith can be measured using ImageJ software (https://imagej.nih.gov/ij/). The thickness-lightness (gray level) calibration is based on a cubed polynomial regression using liths of *Rhabdosphaera* (Jin, Liu, & Zhang, 2019; Figure S2 in Supporting Information S1). Then, the individual coccolith calcite mass (C_M, pg) can be calculated:

$$C_M = 2.7 * A_C * T \quad (5)$$

where A_C is the coccolith area (μm^2), T is the coccolith thickness (μm), and 2.7 is the calcite density (pg μm^{-3}). Here, dozens of coccoliths were measured, giving that the average C_M (and one standard deviation) used in this study was 1.69 (0.46) pg for *E. huxleyi*, 12.41 (4.13) pg for *G. oceanica*, 1.47 (0.78) pg for *F. profunda*, 11.12 (2.28) pg for *Calcidiscus* spp., and 33.63 (13.51) pg for *Helicosphaera* spp. (Figure S3 in Supporting Information S1). Finally, the seawater coccolith calcite concentration of the specific species was determined by the calcite contents from both cells (coccospheres) and detached coccoliths.

3.4. Calcification Degree of *Emiliania huxleyi*

For scanning electron microscopy (SEM) photographing, a small piece of each 25 mm-diameter filter was cut out and mounted on an aluminum stab with conductive carbon tape and coated with gold. Based on the SEM

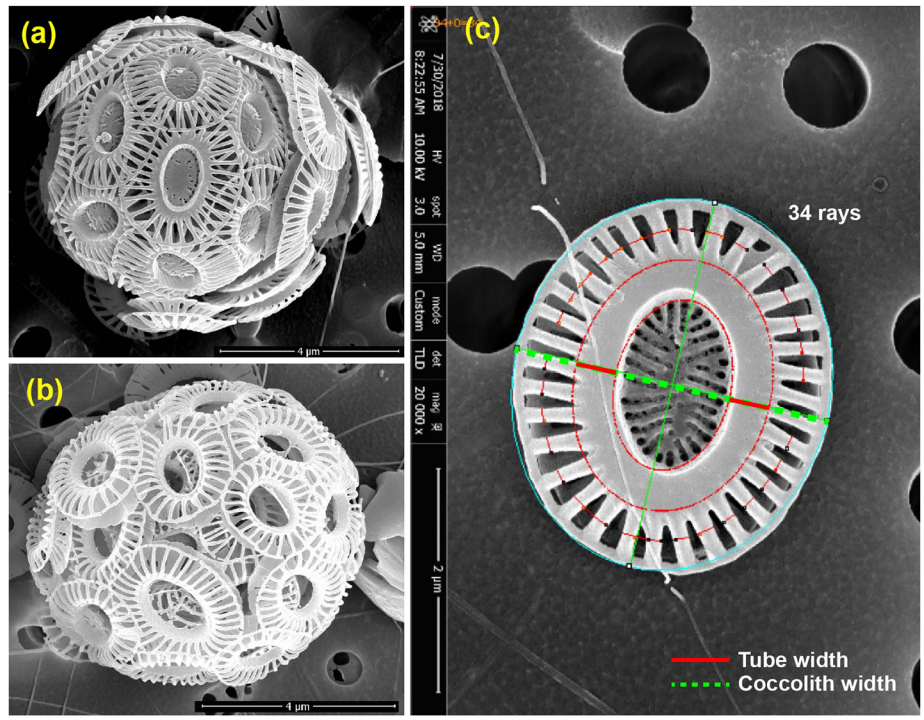

Figure 4. SEM images of *Emiliania huxleyi* morphotypes: type A (a) and type B (b); (c) Distal shield view of a detached *E. huxleyi* type A coccolith. The relative tube width (tube width×2/coccolith width) is used as an index of the calcification degree of *E. huxleyi* (Young et al., 2014).

images, the relative abundance of *E. huxleyi* morphotypes and morphological parameters of detached *E. huxleyi* coccolith were identified and measured, respectively. The morphotypes of the *E. huxleyi* coccosphere in the SCS can be divided into two categories: type A and type B (Figures 4a and 4b). Type A coccoliths are relatively heavily or moderately calcified, with robust elements and a grill-like central area. Type B coccoliths are lightly calcified, with delicate elements, and the central area is open or covered with a thin plate (Hagino et al., 2005; Young et al., 2003). Approximately 40–80 coccospheres were identified in most samples in which *E. huxleyi* coccospheres were abundant. Distal shield coccolith length and relative tube width (twofold tube width divided by coccolith width, Figure 4c) of type A coccoliths were used as indicators for the degree of calcification of *E. huxleyi* (Young et al., 2014). The measuring of coccolith length and tube width were conducted using Coccobiom2-SEM measuring macros (Young et al., 2014; ina.tmsoc.org/nannos/coccobiom/Usernotes.html). Approximately 40 detached coccoliths were photographed at ×10,000 magnification for morphometric measurements in most samples where *E. huxleyi* coccoliths were commonly found.

3.5. Nutrients and Seawater Carbonate Chemistry Measurements

Macronutrient (nitrate + nitrite, phosphate, silicate) concentrations were analyzed at full depth at each station, with a classical colorimetric method using a BRAN-LUEBBE AA3 Autoanalyzer. The detection limits were 0.1 μmol L^{-1} for nitrate + nitrite (NO_3^- + NO_2^-, dissolved inorganic nitrogen, DIN), 0.08 μmol L^{-1} for phosphate (PO_4^{3-}, dissolved inorganic phosphorus, DIP), and 0.16 μmol L^{-1} for silicate (SiO_3^{2-}). Seawater total alkalinity (TA) and dissolved inorganic carbon (DIC) at full depth at each station were determined following the updated Joint Global Ocean Flux Study protocols (Dickson et al., 2007) and measured with an Apollo AlK1 + TA analyzer. DIC was measured with an Apollo AS C-3 DIC analyzer at a precision of 0.1%. TA was measured by potentiometric Gran titration at a precision of 0.1%. Details of the measurement methods were described in Cai et al. (2004). CO_2 CRMs provided by Dr. Dickson's Lab at Scripps Institute of Oceanography were used to calibrate the DIC and TA measurements to an accuracy of ±2 μmol kg^{-1}. The key carbonate chemistry parameters for coccolithophores, such as bicarbonate ion (HCO_3^-), H^+ (pH), aqueous CO_2 (CO_2aq) concentrations, and calcite saturation ($\Omega_{calcite}$), were then calculated using the CO_2sys Excel macro (Pierrot et al., 2006).

3.6. Statistical Analyses

At St. 30 (Figure 2a), a series of CTD casts showed that the DCM depth varied with respect to the sampling time in a day (Figure S4 in Supporting Information S1). That is, the DCM was shallower during the days and was deeper at nights, dawn, and dusk. Thus, it may not be proper to use the environmental variables at a sampling (DCM) depth to describe the environments of the water column. Instead, the environmental parameters at 75 m depth, that is, temperature, DIN, DIP, pH, CO_2aq, HCO_3^-, $\Omega_{calcite}$ at 75 m, were used. For some cases, when DIN and DIP were below detection limits at 75 m at a station, DIN and DIP were noted as zero, or when a water sample at 75 m was not collected at a station, the environmental variables at 75 m were obtained by linear interpolation within the two nearest depths. Principal component analysis (PCA) was performed on these environmental data, so that we could identify the major environmental gradients (PC scores) and which environmental variables represented the major environmental gradients in the study area. In addition, Pearson's *r* correlation was carried out between the biotic data (coccolithophore cell abundances, seawater PIC, indices of *E. huxleyi* calcification degree) and the major environmental gradients (PC scores) and the individual environmental variables (i.e., the environmental data at 75 m) to find their possible linkages. The statistical analyses were conducted using PRIMER-E (v6.0) (Clarke et al., 2014) and PAST (Hammer-Muntz et al., 2001).

4. Results

4.1. An Environmental Gradient Along the Investigated Stations

The macronutrient (DIN, DIP, and silicate) concentrations and seawater carbonate chemistry parameters (TA, DIC, bicarbonate ion, CO_2aq, pH, and $\Omega_{calcite}$) profiles at each station are shown in Figures 5a–5c and Figures 6a–6f, respectively. The DIN and DIP concentrations were below the detection limit in the uppermost waters (upper approximately 25–50 m; Figures 5a and 5b), indicating that the investigated SCS and WP areas were oligotrophic during the investigation season. The DIN and DIP concentrations from all sampling waters were highly correlated, and the DIN:DIP ratios ranged from 5.93 to 16.47, with an average value of 13.97, below the Redfield ratio of 16:1 (Redfield et al., 1963).

Values of the environmental variables at 75 m water depth are shown in Figures 7a–7c and Figures 7e–7h, indicating an environmental gradient along the investigated trajectory. The highest DIN and DIP concentrations at 75 m were observed at the N-SCS stations. The macronutrient concentrations were lower at the NE-SCS stations, and were the lowest or below the detection limits at the WP and B-SCS stations (Figures 7a and 7b). The seawater temperature at 75 m showed a similar pattern as the macronutrients. The lowest temperature was observed at the N-SCS stations, and the highest seawater temperature was at the WP and B-SCS stations (Figure 7c). Although strongly dependent on sampling time (Figure S4 in Supporting Information S1), the DCM (sampling) depth at each station (Figure 7d) still to some extent followed the pattern of macronutrient concentrations at 75 m, with higher water column nutrient levels in relation to shallower DCM depths from St. 12 to St. 37 along the trajectory (Figure 7d). The seawater carbonate chemistry parameters (i.e., $\Omega_{calcite}$, CO_2aq, HCO_3^-, pH) were strongly intercorrelated (Figure 6) and showed a similar pattern as macronutrients and temperature. The highest CO_2aq and HCO_3^- with the lowest $\Omega_{calcite}$ and pH were observed at the N-SCS stations; in comparison, the lowest CO_2aq and HCO_3^- with the highest $\Omega_{calcite}$ and pH were observed at the WP and B-SCS stations (Figures 7e–7h).

4.2. Coccolithophore Cell and Coccolith Concentrations

Total coccolithophore cell concentrations in the DCM layers ranged from approximately 5 to 40 cells mL^{-1} (Figure 8a). This range was comparable with previous investigations in the SCS during the summer seasons (Jin et al., 2016; Sun et al., 2011, 2015). The coccolithophore cells were dominated by *E. huxleyi* at the N- and B-SCS stations; in comparison, more occurrences of *G. oceanica* cells were found at the NE-SCS stations. For the WP stations, the coccolithophore cells were dominated by *A. robusta* (Figure 8a). The detached coccolith concentrations of *E. huxleyi*, *G. oceanica* and *F. profunda* ranged from approximately <50 to 600 coccoliths mL^{-1} (Figure 8b). The geographical (horizontal) distribution pattern of the detached coccoliths of these species followed the distribution of their cells/coccospheres. *E. huxleyi* coccoliths dominated at the N- and B-SCS stations, and more *G. oceanica* coccoliths were found at the NE-SCS stations (Figure 8b). *E. huxleyi* and *F. profunda* coccoliths were highly correlated with their coccosphere concentrations (Figures 8c and 8d), indicating that these suspended coccoliths were directly dropped by their living cells. For *G. oceanica* coccoliths, the

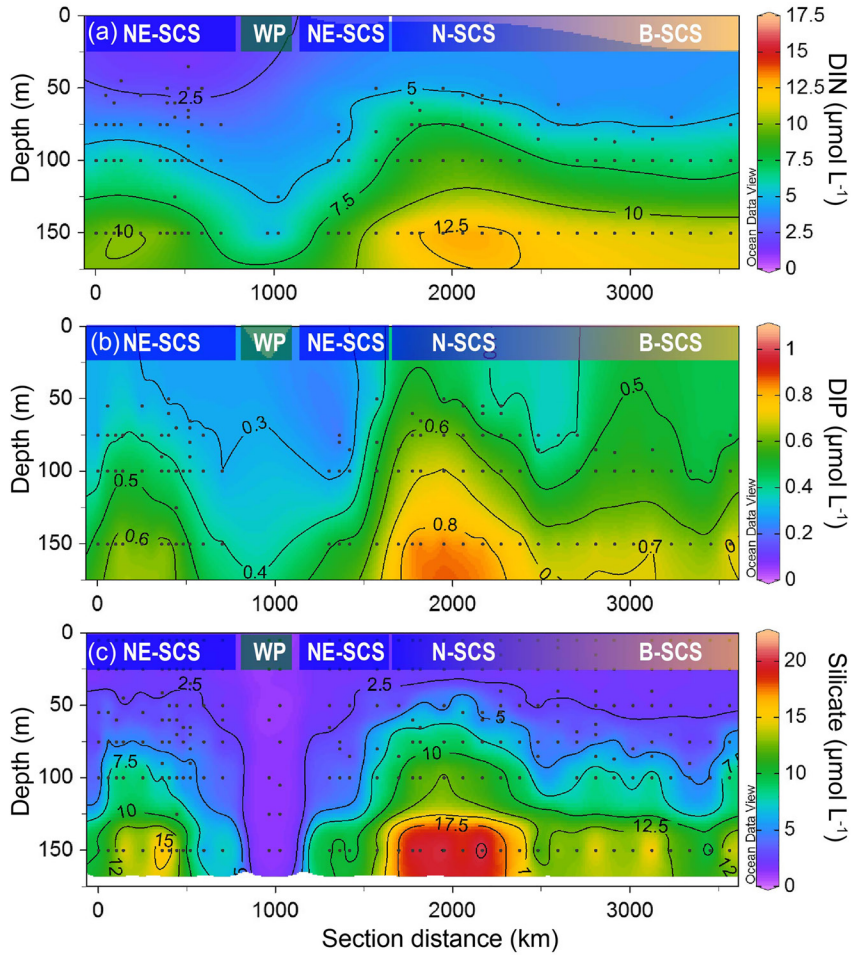

Figure 5. DIN (a), DIP (b), and silicate (c) concentrations in the upper 150 m water column of the investigated stations in the SCS and WP. NE-SCS, northeastern SCS; N-SCS, northern SCS; B-SCS, basin SCS; WP, the Western Pacific.

correlation of detached coccoliths with coccospheres was only observed at the stations excluding St. 1 to 4 which were near the continental slope (Figure 8e). In particular, higher suspended *G. oceanica* coccoliths (100 to >300 coccoliths mL^{-1}) were found in these samples (St. 1 to 4) (Figure 8b). In addition, fossilized coccolith specimens of *Sphenolithus* spp. and large *Reticulofenestra* spp. (>5 μm) were also observed in these samples, suggesting that the "excess" detached *G. oceanica* coccoliths may originate from the lateral transport of the resuspended sediments from the adjacent continental shelf or slope. High *A. robust* cell concentrations (up to 10 cells mL^{-1}) were observed at the oligotrophic WP stations (St. 13 and 14) (Figure 8a), where the sampling depth was more than 100 m (Figures 7a–7d). This species was previously recognized as a lower euphotic zone (LPZ) species such as *F. profunda* in the SCS (Jin et al., 2016). Similar to *F. profunda*, *A. robusta* could be mixotrophic or phagotrophic, as an important nutritional strategy in dysphotic waters (Poulton et al., 2017).

4.3. Coccolith Calcite of the Key Species and Genera, and Their Contribution to Suspended PIC

The investigated seawater PIC concentration ranged from approximately 4,500 to 15,000 pg $CaCO_3$ mL^{-1}, with an average of approximately 9,147 pg $CaCO_3$ mL^{-1} (Figure 9a). This range was comparable and on the same order of magnitude as the suspended seawater PIC concentration detected in the subsurface waters of the tropical-subtropical Atlantic, Indian, and Pacific oceans (Beaufort et al., 2008; Marañón et al., 2016). Here, the seawater coccolith calcite was estimated from the calcite content of *E. huxleyi*, *G. oceanica*, *F. profunda*, *Calcidiscus*, and *Helicosphaera*. The results showed that the contribution of *E. huxleyi* coccoliths to seawater PIC was 6.8% on average for the total stations, and a higher contribution (>10–20%) was found at some stations in the N- and

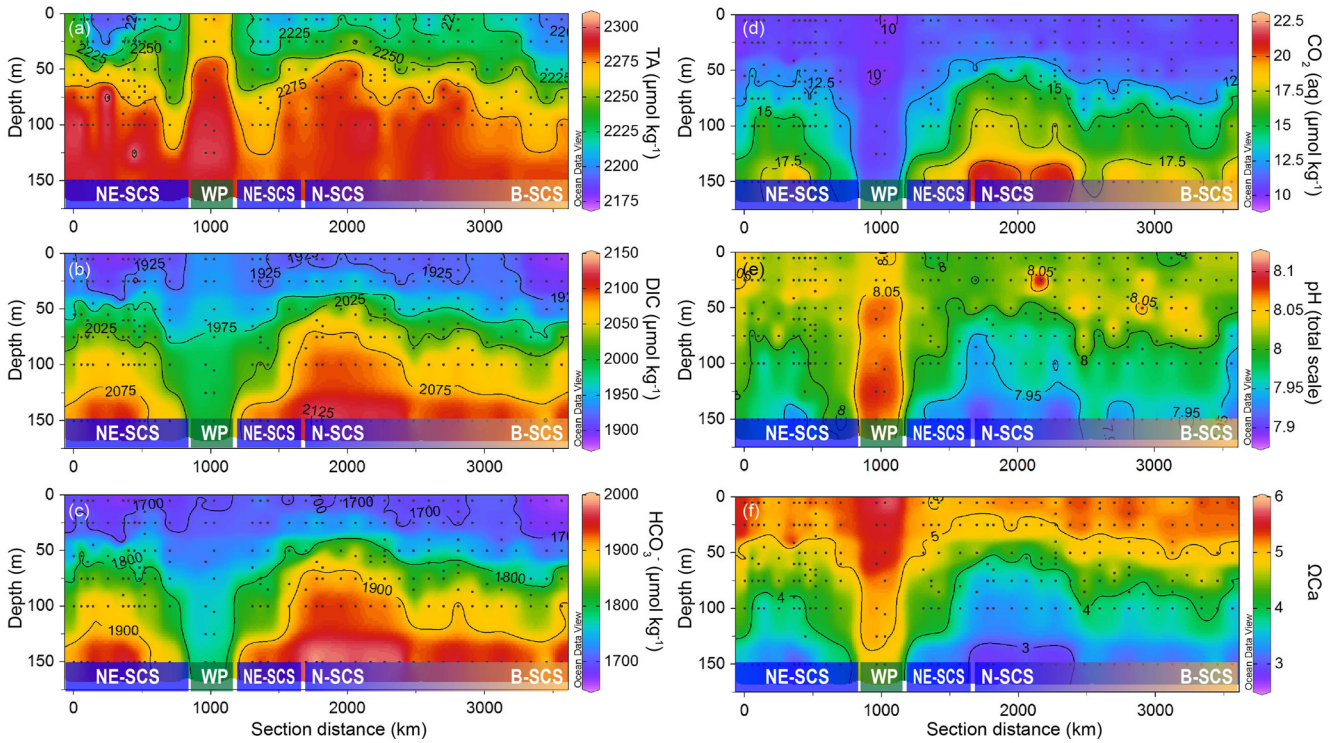

Figure 6. Seawater total alkalinity (TA) (a), dissolved inorganic carbon (DIC) (b), bicarbonate ion concentration (c), aqueous CO_2 concentration (d), pH (total scale, *in situ* temperature) (e), and calcite saturation (Ω_{Ca}) (f) in the upper 150 m water column of the investigated stations in the SCS and WP. NE-SCS, northeastern SCS; N-SCS, northern SCS; B-SCS, basin SCS; WP, the Western Pacific.

B-SCS (Figure 9b). The *G. oceanica* coccoliths on average contributed to 10.6% of the seawater PIC, and their contributions can be more than approximately 20% at some NE-SCS stations (Figure 9c). The average coccolith calcite concentration of these two species was approximately 1,500 pg mL^{-1}, and they totally contributed to approximately 17.4% of the suspended seawater PIC on average. These values were lower than those observed in the subtropical Pacific Ocean (Beaufort et al., 2008). Beaufort et al. (2008) found that Noelaerhabdaceae coccolithophore calcite concentration was on average approximately 2,200 pg mL^{-1}, and contributed to approximately 22% of the seawater PIC inventory. The nannolith calcite concentration of *F. profunda* and their contribution to seawater PIC were highly variable, with an average contribution of 2.7% for the investigated stations (Figure 9d). Finally, *Calcidiscus* + *Helicosphaera* on average contributed to approximately 2.3% of seawater PIC. Higher contributions can be found at the N- and B-SCS stations (Figure 9e). In comparison, although with a lower coccosphere/coccolith number in the coccolithophore assemblage, calcite of these two genera was still found to be one of the major contributors to deep ocean PIC flux in the North Atlantic (Ziveri et al., 2007). The smaller contribution in the SCS may be because they were relatively lightly calcified; that is, the average coccolith mass of both *Calcidiscus* and *Helicosphaera* in the SCS was much lower than those in the North Atlantic (Young & Ziveri, 2000). Finally, the total coccolith calcite contribution of these key species and genera to seawater PIC ranged from 2.5% to 55.2%, with an average of 22.4% for the investigated water samples in the study area.

4.4. Calcification Degree of *Emiliania huxleyi*

A total of 1,081 *E. huxleyi* coccospheres were identified in the SEM images. The relative abundance of type A coccospheres ranged from 54.5% to 97.5% for the investigated samples, with an average relative abundance of 75.5%, indicating type A coccospheres as the dominant morphotype of *E. huxleyi* in the tropical SCS (Figure 10a). A total of 1,048 detached *E. huxleyi* type A coccoliths were photographed for morphometric measurements. The relative tube width (rtw) ranged from approximately 0.15 to 0.3 (Figure 10b), with an average value of 0.21 for the total specimens. The coccolith length of distal shield ranged from approximately 2.5 to 3.5 μm, with an average coccolith length of 3.1 μm of *E. huxleyi* type A (Figure 10c). A very weak correlation was found between rtw

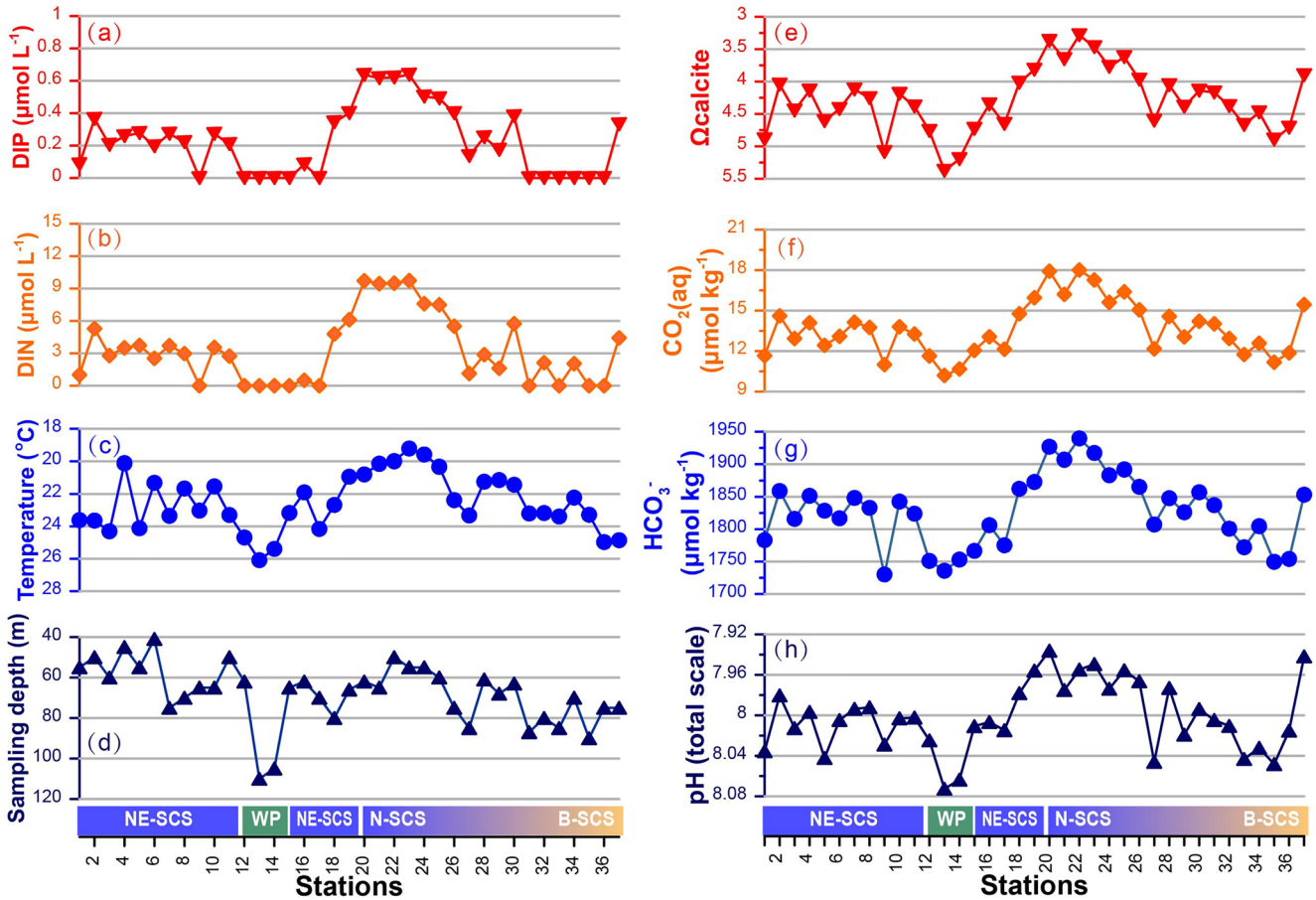

Figure 7. Environmental variables at 75 m water depth (a-c, e-h) showing the environmental gradient along the investigated stations. (a) DIP, (b) DIN, (c) seawater temperature, (d) sampling (DCM) depth, (e) calcite saturation ($\Omega_{calcite}$), (f) aqueous CO_2, (g) bicarbonate ion concentration, (h) pH (total scale, *in situ* temperature).

and coccolith length for the total set of measurements ($r = 0.1$, $p < 0.01$), suggesting an independence of rtw on the coccolith size (Young et al., 2014). In addition, neither of the rtw nor coccolith length showed a strong geographical (horizontal) distribution in the SCS (Figures 10b and 10c). The rtw and coccolith length data measured here were in the same range as the "oceanic *E. huxleyi* populations" that were found in the North Sea (Young et al., 2014).

4.5. Coccolithophore Community in Relation to Environmental Variables

According to the PCA on the environmental variables at 75 m water depth (Figure 7), two principal components (PCs) were extracted, and contributed 81% and 9.7% (totally 90.7%) of the total variance between stations, respectively. PC1 was significantly related to all the environmental variables, and strongly correlated with the DIN, DIN, temperature, pH, $[HCO_3^-]$, CO_2aq, and $\Omega_{calcite}$ ($r > 0.8$, $p < 0.01$) (Table 1). The PCA results reveal that the major environmental gradient along the trajectory can be represented by PC1, which explained the majority (81%) of the total variance along the sampling stations (Figure 7), and PC1 was contributed by macronutrients and all of the carbonate chemistry parameters, which were significantly intercorrelated (Figure 11a). PC2 was a representative of the sampling depth of each station (Table 1). Since, we did not sample water at full depth at each station, PC2 explained only a minor percent (9.7%) of the total variance.

The Pearson correlation analysis showed that *E. huxleyi*, *E. huxleyi* + *G. oceanica* and total coccolithophore cell abundances were significantly related to the major environmental gradient (PC1) along the sampling trajectory (Figures 11b and Table 2). Total cell abundance of the LPZ species (*F. profunda* + *A. robust*) showed a significant relation to PC2 (Figure 11b, Table 2) and a very week positive relation to temperature ($r = 0.31$, $p = 0.057$;

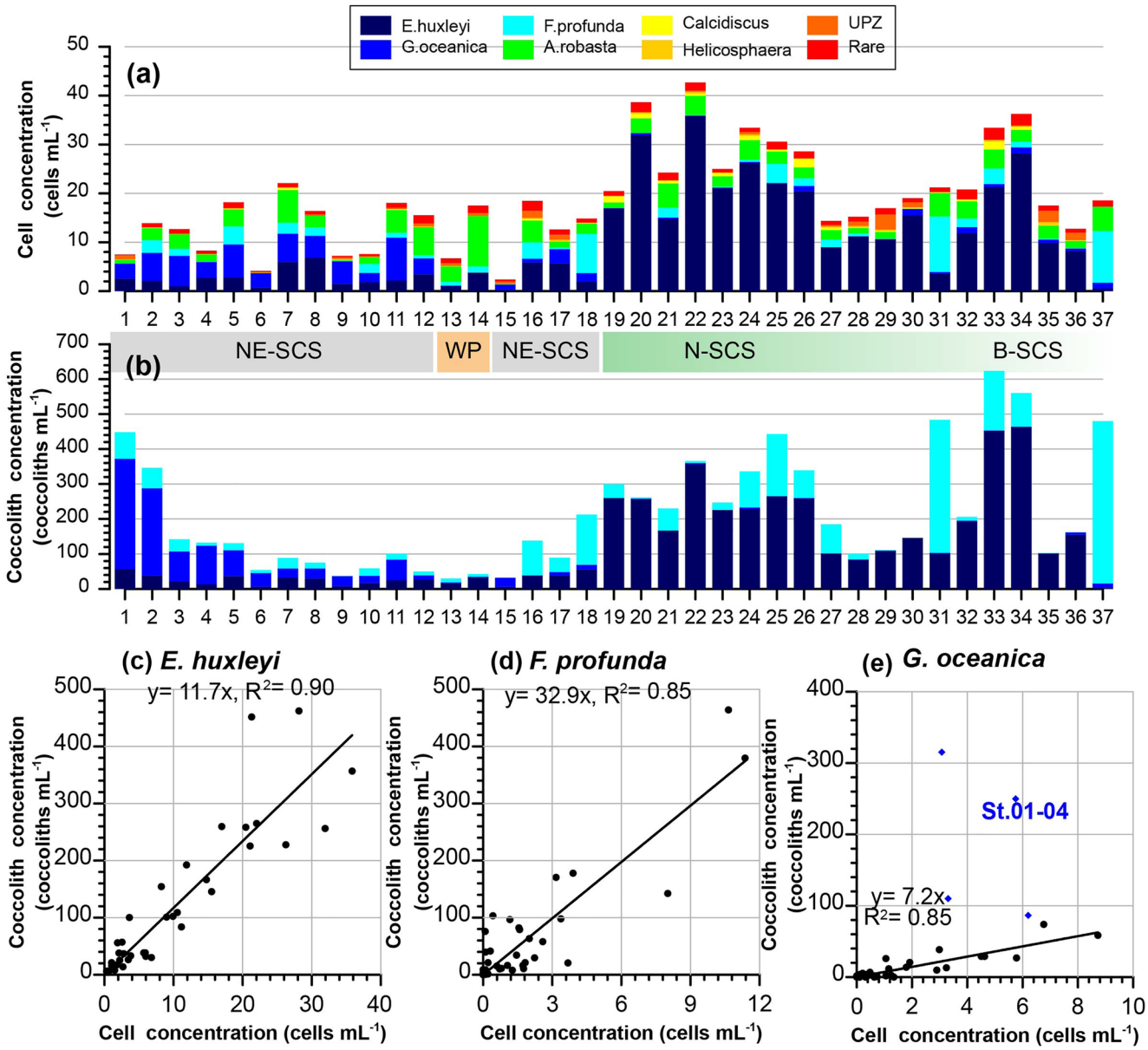

Figure 8. Coccolithophore cell (coccosphere) (a) and detached coccolith (b) concentrations at the investigated stations in the SCS and WP. Scatter plots showing relationships between the detached coccoliths and coccospheres of *E. huxleyi* (c), *F. profunda* (d), and *G. oceanica* (e). UPZ: upper euphotic zone species/genera; Rare: "rare species" group.

Table 2). This may indicate that the cell abundance of the observed LPZ species depends on the sampling depth and, to a lesser extent, the in situ temperature at a station. That is, higher water temperature in deeper waters may favor the inhabitant the LPZ.

5. Discussion

5.1. Insensitivity of *E. huxleyi* Calcification to Carbonate Chemistry

Seawater carbonate chemistry parameters, for example, bicarbonate (HCO_3^-) and carbonate ions ($\Omega_{calcite}$), aqueous CO_2, and H^+ concentrations (pH), are important variables for coccolithophore growth and calcification. The degree of coccolith calcification may directly control coccolith-based calcite production and concentration in seawater. Here, our data showed that the relative abundance of *E. huxleyi* type A and the morphology of

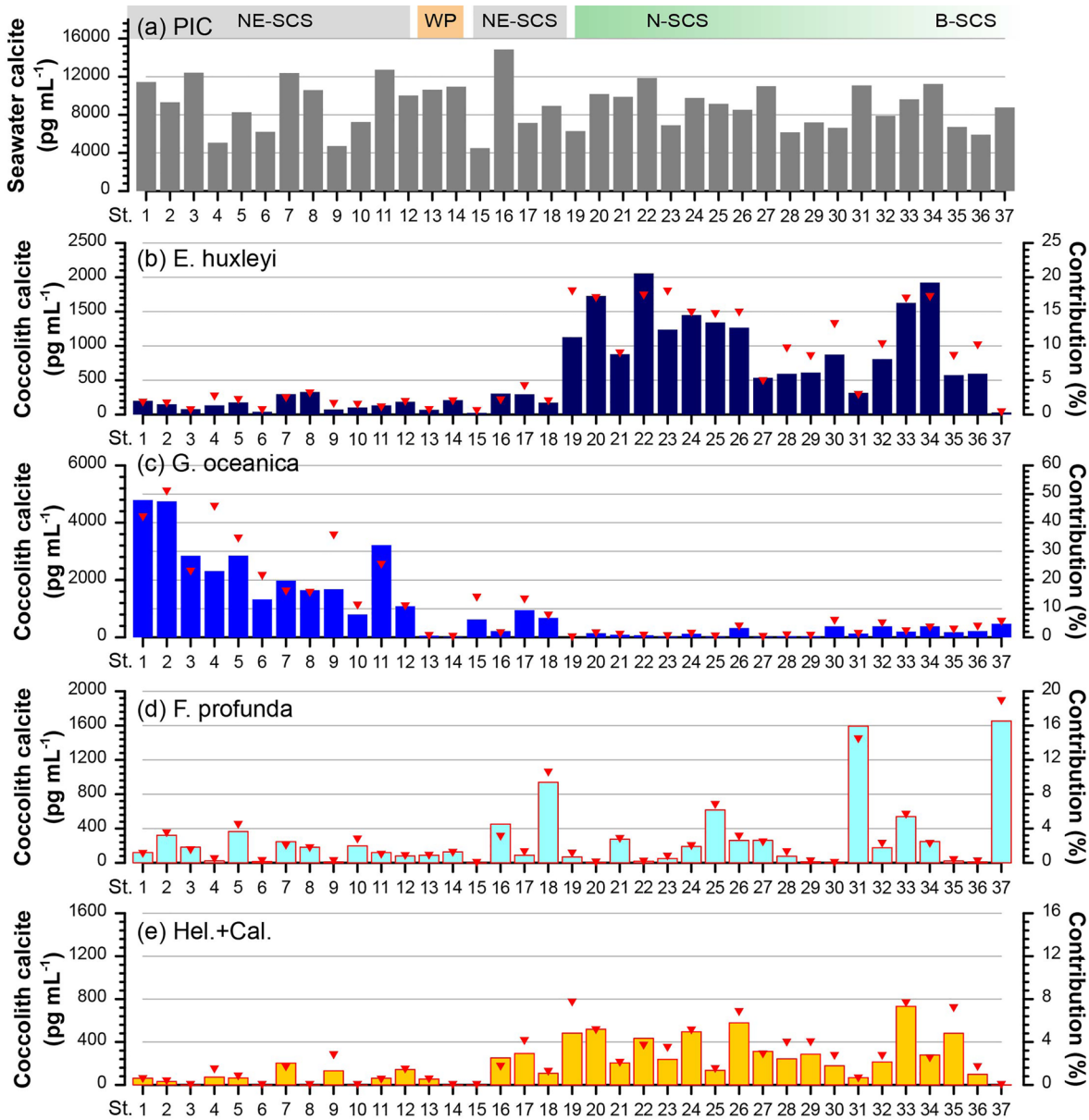

Figure 9. (a) Seawater PIC concentration (pg $CaCO_3$ mL^{-1}) at the investigated stations in the SCS and WP. (b)–(e) Seawater coccolith calcite concentration (pg $CaCO_3$ mL^{-1}) (columns) and their contribution (%) (red triangles) to seawater PIC of *E. huxleyi* (b), *G. oceanica* (c), *F. profunda* (d), and *Helicosphaera* + *Calcidiscus* (e).

coccoliths, that is, coccolith length and rtw, were not related to pH, HCO_3^-, CO_2aq, or $\Omega_{calcite}$ (Table 2), indicating an insensitivity of the *E. huxleyi* calcification degree to the seawater carbonate chemistry. Coccolith distal shield length of *E. huxleyi* type A showed a weak and negative correlation with PC2 ($r = -0.39$, $p = 0.05$), and a very weak and negative correlation with temperature, although it was insignificant ($r = -0.34$, $p = 0.09$; Table 2). That is, a larger *E. huxleyi* size may be related to a deeper water depth and lower temperature. This finding agrees with our previous investigation of the SCS during summer 2014 (Jin et al., 2016). Larger *E. huxleyi* coccoliths found in deeper waters at a station may result from lower cell growth due to a shortage of light availability (Jin et al., 2016). Comparatively, the present results indicated that the degree of *E. huxleyi* coccolith calcification at the DCM layer of each station did not show a significant horizontal change in relation to the major environmental gradient.

Similar findings of the insensitivity of *E. huxleyi* type A coccolith length and rtw to carbonate chemistry have also been reported in the North Sea (Young et al., 2014), where significant changes in the coccolith morphology

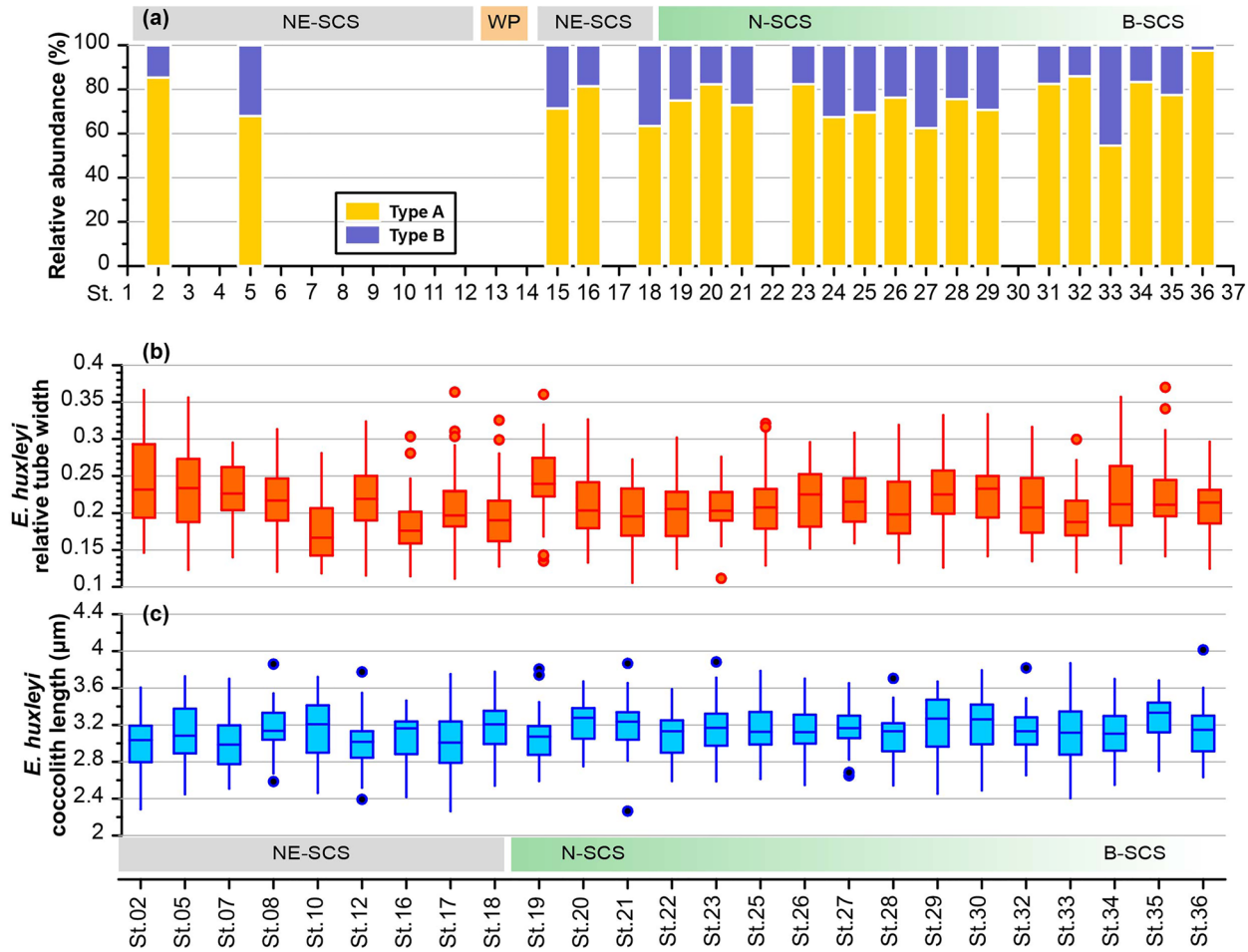

Figure 10. Relative abundance of *E. huxleyi* morphotypes (type A and type B) (a), relative tube width (b) and coccolith length of distal shield (c) of *E. huxleyi* type A coccoliths at the investigated stations in the SCS. Box plots in panels (b) and (c) indicate median, upper and lower quartiles, and outliners.

of *E. huxleyi* type A were suggested to be induced by a genetic variation between the oceanic and neritic populations (Young et al., 2014). In comparison, most of the field investigations in the Southern Ocean revealed that the degree of *E. huxleyi* calcification (indicated by coccolith mass) showed negative relation to seawater CO_2aq/pCO_2 and $\Omega_{calcite}$ (Patil et al., 2022; Saavedra-Pellitero et al., 2019); indeed, the change in *E. huxleyi* calcification degree reflected the morphotypic changes, that is, a southward and latitudinal transition from heavily or moderately calcified type A to lightly calcified morphotypes (B, C, B/C) in the Southern Ocean (Patil et al., 2022; Poulton et al., 2011; Saavedra-Pellitero et al., 2019). However, this kind of morphotypic change was also suggested to be dominantly related to temperature and light, rather than carbon chemistry alone (Charalampopoulou et al., 2016; Saavedra-Pellitero et al., 2019), likely reflecting the environmental plasticity and adaptation of *E. huxleyi* morphotypes.

Our results indicate an insensitive response of the calcification degree of *E. huxleyi* type A, as well as the relative abundance of *E. huxleyi* morphotypes, to carbonate chemistry in the present SCS. This response could be due to the relatively narrow changes or gradients of carbonate chemistry (e.g., pH, Figure 7h) in the SCS, or because the carbonate chemistry was not the first-order limiting factor of coccolithophore calcification for the "snapshot" sampling. However, with a long-term view, an observation showed a decline

Table 1
Principal Component (PC) Analysis Showing the Eigenvectors and Pearson Correlation Coefficients of the Environmental Variables in Relation to PC1 and PC2

Variables	PC1 eigenvectors	PC1 Pearson's r	PC2 eigenvectors	PC2 Pearson's r
S. depth	0.23	**0.58**	−0.89	**−0.79**
DIN	−0.37	**−0.95**	−0.16	−0.14
DIP	−0.37	**−0.95**	−0.13	−0.12
Temp.	0.32	**0.81**	−0.31	−0.27
pH	0.36	**0.91**	0.09	0.08
HCO_3^-	−0.38	**−0.97**	−0.13	−0.12
CO_2aq	−0.39	**−0.98**	−0.17	−0.15
$\Omega_{calcite}$	0.38	**0.98**	0.11	0.10

Note. S. depth: sampling depth. Bold numbers indicate $p < 0.01$.

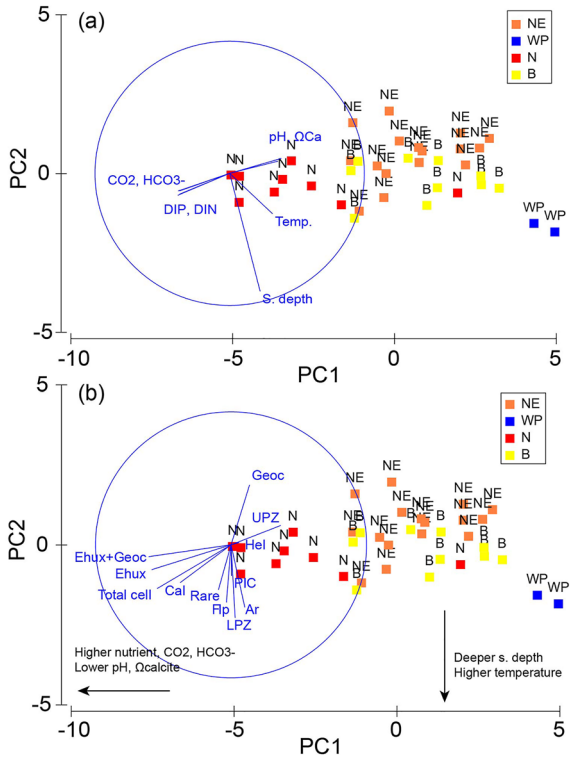

Figure 11. Principal component (PC) ordinations plotted versus the eigenvectors of environmental variables (a) showing the environmental gradients along the sampling stations (NE, northeastern SCS; WP, the Western Pacific; N, northern SCS; B, basin SCS); and the Pearson coefficient vectors (Pearson correlation between PC1 and PC2) of coccolithophore cell abundances and seawater PIC (b) showing the control of environmental gradients on the coccolithophore community. Ehux: *E. huxleyi*; Geoc: *G. oceanica*; Flp: *F. profunda*, Ar: *A. robusta*, LPZ: lower euphotic zone groups; UPZ: upper euphotic zone groups; Rare: "rare" species; Cal: *Calcidiscus* spp., Hel: *Helicosphaera* spp.

in the coccolith calcification degree (indicated by coccolith mass of *E. huxleyi*) from 1993 to 2005 A. D. in response to ongoing ocean acidification in the Mediterranean Sea (Meier et al., 2014). The persistence of ocean acidification may likely select lightly calcified morphotypes (e.g., type B group of *E. huxleyi*) as calcite producers, lowing their inorganic carbon production in the future ocean.

5.2. Controls of Nutrient Level on Coccolithophore Abundance in the Water Column

The data showed that the cell abundances of *E. huxleyi* and *E. huxleyi* + *G. oceanica* were significantly related to the major environmental gradient (PC1) along the investigated trajectory (Table 2; Figure 11b), and PC1 was mathematically contributed by the nutrient level of the water column (DIN and DIP at 75 m), carbonate chemistry (pH, HCO_3^-, CO_2aq, and $\Omega_{calcite}$ in Figure 7), and temperature (Table 1). Since *E. huxleyi* and *G. oceanica* were the predominant cells in the DCM layers in the SCS (Figure 8a), the total cell abundance of coccolithophore naturally showed a significant correlation with PC1. Here, the coccolithophore cells were also negatively related to temperature (Table 2), whereas, the temperature limitation on phytoplankton growth follows an exponential function (Nissen et al., 2018), as coccolithophores should grow faster with higher temperature. Therefore, temperature should not be a controlling factor on coccolithophore growth and abundance here. Although the PAR/PAR_0 data were not available at each station due to some CTD casts at night, the 10% surface irradiance depth along the trajectory was approximately 50–70 m, generally in line with the DCM depth at the SCS stations (Figures 3d and 3f). We speculated that autotrophic phytoplankton growth would not be limited by light at DCM, where PAR could be approximately 200 μmol photons m^{-2} s^{-1} (based on a regular surface PAR of approximately 2000 μmol photons m^{-2} s^{-1} during the summer (Jin et al., 2016)). Such an amount of photon flux is above a critical irradiance threshold or interval (25–150 μmol photons m^{-2} s^{-1}) for coccolithophore blooms in the modern ocean (Iglesias-Rodríguez et al., 2002).

Since the macronutrients and carbonate chemistry parameters were highly intercorrelated, it is difficult to separate which parameter(s) was(were) key for coccolithophore growth in the SCS. For carbonate chemistry, lower pH (higher $[H^+]$) and $\Omega_{calcite}$ are detrimental for coccolithophore calcification, and higher HCO_3^- and CO_2 can facilitate coccolithophore growth, as they are the important carbon sources for photosynthesis and calcification (Bach et al., 2013, 2015). Here, coccolithophore cell abundances were positively related to HCO_3^- and CO_2aq (Table 2), suggesting a possible carbon limitation for coccolithophore growth. Most culturing studies have shown that regardless of whether organic carbon production by coccolithophores positively or negatively responds to increased CO_2, the response of inorganic carbon (coccoliths) production should be negative, leading to a decline in the inorganic to organic carbon production rate (reviewed by Meyer & Riebesell, 2015). Hence, it can be inferred that if coccolithophore growth was controlled by ambient CO_2 (i.e., a possible CO_2 limitation on coccolithophore growth), the degree of coccolith calcification would decrease. However, the degree of coccolith calcification (i.e., *E. huxleyi*) was found to be insensitive to the carbonate chemistry parameters (Table 2), logically indicating that carbon limitation was not critical for coccolithophore growth and their abundance change in seawater for the present investigation in the SCS. Accordingly, we propose a major control of the nutrient level of the water column on the basin-wide and horizontal change in the Noelaerhabdaceae coccolithophore (*E. huxleyi* + *G. oceanica*) cell abundance in the SCS and WP.

5.3. Influences of Macronutrient Structures on *E. huxleyi* and *G. oceanica*

The abundances of *E. huxleyi* and total Noelaerhabdaceae coccolithophores (*E. huxleyi* + *G. oceanica*) were controlled by the nutrient level of the water column in the SCS and WP; however, *G. oceanica* alone did not

Table 2
Pearson Correlation Showing the Coefficients Between the Environmental Variables (and Gradients: PC1 and PC2) and Coccolithophore Cell Abundance, Seawater PIC, and Degree of Emiliania huxleyi Calcification

	S. depth	DIN	DIP	Temp.	pH	HCO_3^-	CO_2aq	$\Omega_{calcite}$	PC1	PC2
Cell abundance										
Ehux	−0.12	**0.62**	**0.54**	**−0.60**	**−0.44**	**0.57**	**0.60**	**−0.60**	**−0.58**	−0.19
Geoc	−0.40	−0.14	−0.11	0.28	0.14	−0.14	−0.21	0.19	0.14	**0.45**
Ehux + Geoc	−0.24	**0.65**	**0.57**	**−0.58**	**−0.45**	**0.59**	**0.61**	**−0.61**	**−0.61**	−0.09
Flp	0.27	−0.03	−0.01	0.23	−0.18	0.14	0.14	−0.16	−0.03	**−0.43**
Ar	0.39	−0.01	−0.02	0.30	0.12	−0.01	−0.02	0.03	0.10	**−0.47**
LPZ	0.39	−0.03	−0.02	0.31	−0.06	0.10	0.09	−0.10	0.03	**−0.55**
UPZ	0.16	−0.41	−0.36	0.10	0.36	−0.40	−0.39	0.37	0.37	0.15
Rare	0.23	0.14	0.05	−0.02	−0.06	0.14	0.17	−0.20	−0.09	−0.34
Total cell	−0.03	**0.58**	**0.51**	**−0.42**	**−0.43**	**0.58**	**0.60**	**−0.61**	**−0.54**	−0.33
Cal	0.06	0.40	0.38	−0.35	−0.32	0.38	0.40	−0.40	−0.37	−0.28
Hel	0.10	−0.09	−0.10	−0.13	0.10	−0.10	−0.05	0.02	0.06	0.02
Seawater PIC										
PIC	0.14	0.03	0.04	0.17	0.08	0.11	0.05	−0.06	0.00	−0.23
Degree of Ehux calcification										
Type A%	−0.14	−0.02	−0.10	0.14	−0.19	−0.04	0.07	−0.06	−0.02	0.07
DSL	0.34	0.19	0.18	−0.34	0.01	0.14	0.09	−0.09	−0.12	−0.39
RTW	−0.07	0.01	−0.01	0.25	0.06	−0.04	−0.08	0.11	0.07	0.02

Note. S. depth, sampling depth; Ehux, *E. huxleyi*; Geoc, *G. oceanica*; Flp, *F. profunda*; Ar, *A. robusta*; LPZ, lower euphotic zone groups; UPZ, upper euphotic zone groups; Rare, "rare" species; Cal, *Calcidiscus* spp.; Hel, *Helicosphaera* spp.; DSL, coccolith length of distal shield; RTW, relative tube width. Bold numbers indicate significant correlations ($p < 0.01$).

show a significant relation to the macronutrient concentrations (Table 2; Figure 11b). A higher occurrence of *G. oceanica* was only observed at the NE-SCS stations, indicating a possible biogeographical control. Since the coccolith calcite content of *G. oceanica* was much greater than that of *E. huxleyi* (Young & Ziveri, 2000; Figure S3 in Supporting Information S1), the ecology and biogeography of *G. oceanica* should be important for the Noelaerhabdaceae coccolith calcite distribution in seawater.

The biogeographic distribution of the Noelaerhabdaceae coccolithophores reveals that the relative ratios of *E. huxleyi* to *G. oceanica* coccoliths in seafloor sediments increase with further distance to the coast, as has long been observed in the China marginal seas (Cheng & Wang, 1997). A sediment trap study in the northern SCS also showed their distinct phenology of them, as *G. oceanica* cells are produced in December with diatoms, and *E. huxleyi* cells are produced in late February and early March after diatom blooms (Jin, Liu, Zhao, et al., 2019). An explanation of these results may be due to the particularly higher nutrient affinity of *G. oceanica* than *E. huxleyi* (Andruleit et al., 2003; Andruleit & Rogalla, 2002; Jin, Liu, Zhao, et al., 2019). Phytoplankton growth succession and the competition of coccolithophores with diatoms are expected to govern the biogeography and phenology of coccolithophores in oceans worldwide (Hopkins et al., 2015). We may infer that the competition of coccolithophores and diatoms would likely control the biogeographic distribution of the Noelaerhabdaceae coccolithophores in the SCS.

Here, we used the residual nitrate potential growth (RNPG) model (Balch et al., 2016) of diatoms to describe the potential competition of coccolithophores with diatoms and evaluate the influences of macronutrient structure (DIN and silicate distributions) on the ecology of these two coccolithophore species. The RNPG model has been previously introduced to explain the biogeographic distribution of coccolithophores and their competition with diatoms in the Southern Ocean (Balch et al., 2016). RNPG was calculated following Equations 6 to 8 (Balch et al., 2016):

$$\mathrm{RNPG} = \mu_N - \mu_{Si} \quad (6)$$

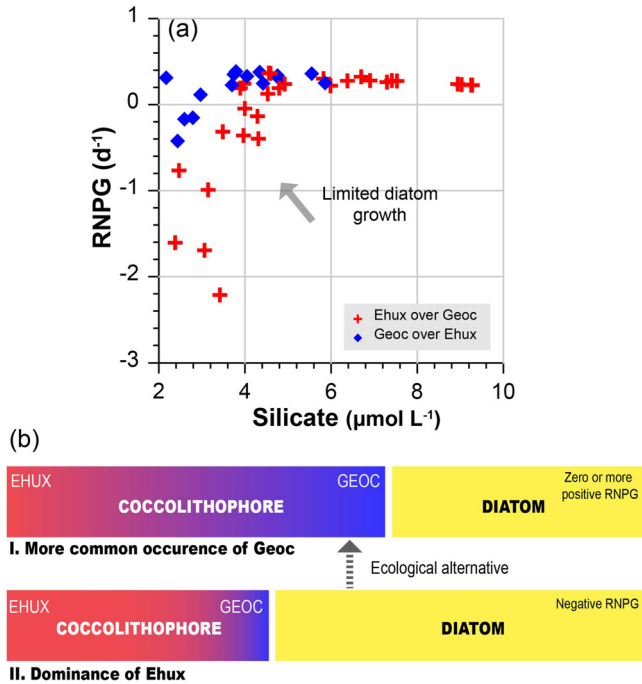

Figure 12. (a) RNPG-plotted versus silicate concentration of the 75 m upper water column in the SCS. More positive RNPG and lower silicate indicate a limited diatom growth. (b) A schematic showing the ecological succession of coccolithophores and diatoms. We propose that when diatom growth was limited by silicate, their ecological niche may be substituted by *G. oceanica*, which shows a greater affinity for nutrients than *E. huxleyi*.

$$\mu_{\mathrm{N}} = \mu_{\max}\,(N/(K_{s-N}+N)) \tag{7}$$

$$\mu_{\mathrm{Si}} = \mu_{\max}((Si-Si_0)/(K_{s-\mathrm{Si}}+(Si-Si_0)) \tag{8}$$

where, μ_{N} and μ_{Si} are the nitrate-based and silicate-based growth rates for diatoms, respectively; $\mu_{\max}$ is the maximum growth rate; $K_{s\text{-N}}$ and $K_{s\text{-Si}}$ are the half-saturation coefficients of DIN and silicate; and Si_0 is the residual silicate concentration required for diatoms (Balch et al., 2016). Here, the maximum growth rate $\mu_{\max}$ and half-saturation coefficients K_s were constants taken from Nissen et al. (2018). N and Si are the *in situ* measured DIN and silicate concentrations.

Based on the shipboard measured nutrient data of the upper 75 m water column, the calculated RNPG varied from −2.18 to 0.41 days^{-1} for diatoms (Figure 12a). In addition, the numbers of *G. oceanica* exceeded *E. huxleyi* at the stations where the RNPG was positive or nearly zero and silicate concentrations were lower (Figure 12a). We propose that diatom growth was potentially limited by the seawater silicate concentration when RNPG was more positive, and silicate was lower. However, we still note that the RNPG here was only a function of the local nutrient concentrations (i.e., DIN and silicate concentrations). Indeed, $\mu_{\max}$ and K_s should change with respect to local eutrophic conditions and diatom species (Balch et al., 2016; Paasche, 1973). A further understanding of the RNPG may require more field investigations and culture studies concerning diatom physiology in the SCS.

If *G. oceanica* was as an effective nutrient assimilator as diatoms, which could be evidenced by the similar phenology of *G. oceanica* and diatoms during the productive seasons in the SCS (Jin, Liu, Zhao, et al., 2019), the ecological niche of diatoms would likely be substituted by *G. oceanica*, when diatom growth was potentially limited by silicate (Figure 12b). Hence, more occurrences of *G. oceanica* could be found in the more positive RNPG waters. As above, we suggest the dependence of the macronutrient structure (DIN and silicate distributions) on the biogeographic distribution of *G. oceanica* and *E. huxleyi*, which govern the Noelaerhabdaceae coccolith calcite concentrations in the SCS.

5.4. Contribution of Coccolith Calcite to Seawater PIC

Our results showed that the key species/genera on average contributed to approximately 22% of seawater PIC in the DCM layers at the investigated stations. The seawater PIC concentration here did not show any significant correlations with the environmental variables (Table 2; Figure 11b), indicating the complexity of sources to seawater PIC. Only <18% of the suspended PIC standing stock at the DCM layers was contributed by the Noelaerhabdaceae coccolithophores (*E. huxleyi* and *G. oceanica*), nevertheless, we still note that Noelaerhabdaceae coccolithophores should be more productive, as shown by their massive detached coccoliths in water samples (Figure 8b). A higher seawater coccolith concentration can reflect a higher coccolith detachment rate and hence a higher growth rate of the Noelaerhabdaceae coccolithophores, ensuring that they are the dominant calcite producers as seen in the deeper water column and seafloor sediments in the SCS (Jin, Liu, Zhao, et al., 2019). It is likely that other coccolithophore groups still contribute a certain amount of calcite to the PIC inventory. For example, the seawater PIC did show a significantly weak correlation with the cell abundance of the "rare" species group ($r = 0.41$, $p = 0.01$) and a significant correlation with *A. robusta* ($r = 0.62$, $p < 0.01$). Furthermore, other non-coccolith carbonate particles should also be additional sources for seawater PIC, that is, the contribution of other calcifiers such as juvenile foraminifers and calcareous dinoflagellates, and abiotic particles such as terrestrial lithogenic calcium carbonate (Daniels et al., 2012). This means that most of the seawater PIC standing stock in the oligotrophic tropical oceans can be recalcitrant, with potentially longer turnover time in the water column. This fact has been confirmed by a series of studies in the past. For instance, the seawater PIC turnover time was approximately 7 days for the most productive waters in the Patagonian shelf during a coccolithophore (*E. huxleyi*)

bloom (Poulton et al., 2013), and comparatively, the turnover time of PIC showed a wide range, from 20 to even >100 days in oligotrophic tropical oceans (Liu et al., 2020; Marañón et al., 2016).

The satellite-based monthly surface PIC during July 2018 in the open SCS ranged from 0.01 to 0.03 mmol C m^{-3} (1,000 to 3,000 pg $CaCO_3$ mL^{-1}; Figure 2c), indicating an extremely low surface PIC concentration. Comparatively, the measured average PIC concentrations in the DCM layers of the SCS were several-fold higher than the satellite-based data, and the subsurface PIC concentrations did not match with the surface data. The decoupling of the satellite-based surface and *in situ* measured subsurface PIC data markedly reflected the systematic errors between these two methods and was due to the highly variable and multisourced subsurface PIC in the oligotrophic waters. Furthermore, since only approximately 1/5 of the PIC standing stock is vigorous for carbonate cycling in the water column, and this portion of PIC which is mostly contributed by Noelaerhabdaceae coccolithophores relies on local nutrient levels and structure (DIN and silicate distributions), we highlight the importance of field investigations in oligotrophic areas for evaluating global inorganic carbon production and their export to deep oceans.

6. Summary

In the present study, we investigated the seawater coccolithophore and coccolith abundances, degree of calcification of *E. huxleyi*, and suspended seawater PIC concentrations in the DCM layer at 35 stations in the SCS and 2 stations in the WP during a cruise in summer 2018. The results demonstrated that the geographic (horizontal) distribution of Noelaerhabdaceae coccolithophore (*E. huxleyi* + *G. oceanica*) cell abundance in the DCM layer was controlled by the nutrient level of the water column. And in particular, the relative occurrence of *E. huxleyi* and *G. oceanica* can be linked to the macronutrient distribution of DIN and silicate. The calcification degree of *E. huxleyi* type A coccolith did not show a remarkable geographic distribution for the investigated areas in the SCS, and was insensitive to seawater carbonate chemistry. Therefore, the specific coccolith calcite in seawater should mostly follow their cell and detached coccolith abundance in the seawater.

The suspended seawater PIC concentrations in the DCM layer ranged from approximately 4,500 to 15,000 pg $CaCO_3$ mL^{-1}, with an average of approximately 9,147 pg $CaCO_3$ mL^{-1} ($\times 10^{-6}$ mmol C m^{-3}) for the investigated waters. Noelaerhabdaceae coccolithophores contributed to a small portion (<18% on average) of the total PIC standing stock in the DCM layer, indicating the multiple sources of the highly variable suspended PIC in the subsurface of oligotrophic waters. Noelaerhabdaceae coccolithophores are the most productive group and play significant roles in vertical $CaCO_3$ transport in water column due to their shorter PIC turnover time in surface water. Our results show a strong dependance of Noelaerhabdaceae coccolithophores on local environments (i.e., macronutrient concentration and structure in the SCS), highlighting the importance of field investigations in oligotrophic areas for evaluating global inorganic carbon production and their export to deep oceans.

Conflict of Interest

The authors declare no conflicts of interest relevant to this study.

Data Availability Statement

The nutrient data can be acquired at PANGAEA (https://doi.pangaea.de/10.1594/PANGAEA.939374). The coccolithophore cell and coccolith abundances, coccolith calcite, and seawater PIC data are available at National Tibetan Plateau Data Center (https://doi.org/10.11888/Ocean.tpdc.272168).

Acknowledgments
Data and samples were collected onboard R/V TAN KAH KEE (TKK), implementing the open research cruise NORC2018-05 supported by National Natural Science Foundation of China (NSFC) Ship-Time Sharing Project (project number: 41749905). The authors appreciate the

References

Andruleit, H., & Rogalla, U. (2002). Coccolithophores in surface sediments of the Arabian Sea in relation to environmental gradients in surface waters. *Marine Geology*, *186*(3), 505–526. https://doi.org/10.1016/s0025-3227(02)00312-2

Andruleit, H., Stäger, S., Rogalla, U., & Čepek, P. (2003). Living coccolithophores in the northern Arabian sea: Ecological tolerances and environmental control. *Marine Micropaleontology*, *49*(1), 157–181. https://doi.org/10.1016/s0377-8398(03)00049-5

Bach, L. T., Mackinder, L. C., Schulz, K. G., Wheeler, G., Schroeder, D. C., Brownlee, C., & Riebesell, U. (2013). Dissecting the impact of CO_2 and pH on the mechanisms of photosynthesis and calcification in the coccolithophore *Emiliania huxleyi*. *New Phytologist*, *199*(1), 121–134. https://doi.org/10.1111/nph.12225

crew of R/V TKK and the contribution of Dr. Weifang Chen (MEL, Xiamen University) who was the chief scientist aboard the NORC2018-05 cruise. The date of nutrients and carbonate system were provided by the Ocean Carbon Group led by Dr. Minhan Dai. We greatly thank Tao Huang, Lifang Wang, Ying Gao, Faisal Hamzah, Wei Yang, Yan Li, and Yanping Xu at Xiamen University for the nutrient and carbonate sample collection and analysis. This study was financed by National Key Research and Development Program of China (2018YFE0202400), and by grants from NSFC (42176060, 41930536).

Bach, L. T., Riebesell, U., Gutowska, M. A., Federwisch, L., & Schulz, K. G. (2015). A unifying concept of coccolithophore sensitivity to changing carbonate chemistry embedded in an ecological framework. *Progress in Oceanography*, *135*, 125–138. https://doi.org/10.1016/j.pocean.2015.04.012

Balch, W. M. (2018). The ecology, biogeochemistry, and optical properties of coccolithophores. *Annual Review of Marine Science*, *10*(1), 71–98. https://doi.org/10.1146/annurev-marine-121916-063319

Balch, W. M., Bates, N. R., Lam, P. J., Twining, B. S., Rosengard, S. Z., Bowler, B. C., et al. (2016). Factors regulating the Great calcite Belt in the Southern Ocean and its biogeochemical significance. *Global Biogeochemical Cycles*, *30*(8), 1124–1144. https://doi.org/10.1002/2016gb005414

Balch, W. M., Bowler, B. C., Drapeau, D. T., Lubelczyk, L. C., & Lyczkowski, E. (2018). Vertical distributions of coccolithophores, PIC, POC, Biogenic Silica, and chlorophyll a throughout the global ocean. *Global Biogeochemical Cycles*, *32*(1), 2–17. https://doi.org/10.1002/2016gb005614

Balch, W. M., Drapeau, D. T., Bowler, B. C., Lyczskowski, E., Booth, E. S., & Alley, D. (2011). The contribution of coccolithophores to the optical and inorganic carbon budgets during the Southern Ocean Gas Exchange Experiment: New evidence in support of the "Great Calcite Belt" hypothesis. *Journal of Geophysical Research*, *116*, C00F06. https://doi.org/10.1029/2011jc006941

Balch, W. M., Gordon, H. R., Bowler, B. C., Drapeau, D. T., & Booth, E. S. (2005). Calcium carbonate measurements in the surface global ocean based on Moderate-Resolution Imaging Spectroradiometer data. *Journal of Geophysical Research*, *110*, C07001. https://doi.org/10.1029/2004jc002560

Balestrieri, C., Ziveri, P., Grelaud, M., Mortyn, P. G., & Agnini, C. (2021). Enhanced *E. huxleyi* carbonate counterpump as a positive feedback to increase deglacial pCO_2sw in the Eastern Equatorial Pacific. *Quaternary Science Review*, *260*, 106921. https://doi.org/10.1016/j.quascirev.2021.106921

Beaufort, L. (2005). Weight estimates of coccoliths using the optical properties (birefringence) of calcite. *Micropaleontology*, *51*(4), 289–297. https://doi.org/10.2113/gsmicropal.51.4.289

Beaufort, L., Couapel, M., Buchet, N., Claustre, H., & Goyet, C. (2008). Calcite production by coccolithophores in the south east Pacific Ocean. *Biogeosciences*, *5*(4), 1101–1117. https://doi.org/10.5194/bg-5-1101-2008

Boeckel, B., & Baumann, K. H. (2008). Vertical and lateral variations in coccolithophore community structure across the subtropical frontal zone in the South Atlantic Ocean. *Marine Micropaleontology*, *67*(3), 255–273. https://doi.org/10.1016/j.marmicro.2008.01.014

Bollmann, J. (2014). Technical Note: Weight approximation of coccoliths using a circular polarizer and interference colour derived retardation estimates - (The CPR Method). *Biogeosciences*, *11*(7), 1899–1910. https://doi.org/10.5194/bg-11-1899-2014

Bollmann, J., Cortés, M. Y., Haidar, A. T., Brabec, B., Close, A., Hofmann, R., et al. (2002). Techniques for quantitative analyses of calcareous marine phytoplankton. *Marine Micropaleontology*, *44*(3), 163–185. https://doi.org/10.1016/s0377-8398(01)00040-8

Broecker, W., & Clark, E. (2009). Ratio of coccolith $CaCO_3$ to foraminifera $CaCO_3$ in late Holocene deep sea sediments. *Paleoceanography*, *24*(3). https://doi.org/10.1029/2009pa001731

Cai, W. J., Dai, M. H., Wang, Y. C., Zhai, W. D., Huang, T., Chen, S. T., et al. (2004). The biogeochemistry of inorganic carbon and nutrients in the Pearl River estuary and the adjacent Northern South China Sea. *Continental Shelf Research*, *24*(12), 1301–1319. https://doi.org/10.1016/j.csr.2004.04.005

Charalampopoulou, A., Poulton, A. J., Bakker, D. C., Lucas, M. I., Stinchcombe, M. C., & Tyrrell, T. (2016). Environmental drivers of coccolithophore abundance and calcification across Drake passage (Southern Ocean). *Biogeosciences*, *13*(21), 5917–5935. https://doi.org/10.5194/bg-13-5917-2016

Chen, Y. L. L., Chen, H. Y., & Chung, C. W. (2007). Seasonal variability of coccolithophore abundance and assemblage in the northern South China Sea. *Deep Sea Research Part II: Topical Studies in Oceanography*, *54*(14–15), 1617–1633. https://doi.org/10.1016/j.dsr2.2007.05.005

Cheng, X., & Wang, P. (1997). Controlling factors of coccolith distribution in surface sediments of the China seas: Marginal sea nannofossil assemblages revisited. *Marine Micropaleontology*, *32*, 155–172. https://doi.org/10.1016/s0377-8398(97)00018-2

Clarke, K. R., Gorley, R. N., Somerfield, P. J., & Warwick, R. M. (2014). *Change in marine communities: An approach to statistical analysis and interpretation* (3rd ed.). PRIMER-E.

Daniels, C. J., Tyrrell, T., Poulton, A. J., & Pettit, L. (2012). The influence of lithogenic material on particulate inorganic carbon measurements of coccolithophores in the Bay of Biscay. *Limnology & Oceanography*, *57*(1), 145–153. https://doi.org/10.4319/lo.2012.57.1.0145

Dickson, A. G., & Goyet, C. (1994). *Handbook of methods for the analysis of the various parameters of the carbon dioxide system in sea water. Version 2 (No. ORNL/CDIAC-74)*. Oak Ridge National Lab.

Dickson, A. G., Sabine, C. L., & Christian, J. R. (2007). *Guide to Best Practices for Ocean CO_2 Measurements* (Vol. 3, p. 191). PICES Special Publication.

Duchamp-Alphonse, S., Siani, G., Michel, E., Beaufort, L., Gally, Y., & Jaccard, S. L. (2018). Enhanced ocean-atmosphere carbon partitioning via the carbonate counter pump during the last deglacial. *Nature Communications*, *9*(1), 2396. https://doi.org/10.1038/s41467-018-04625-7

Fernando, A. G. S., Peleo-Alampay, A. M., & Wiesner, M. G. (2007). Calcareous nannofossils in surface sediments of the eastern and Western South China Sea. *Marine Micropaleontology*, *66*(1), 1–26. https://doi.org/10.1016/j.marmicro.2007.07.003

Fuertes, M. Á., Flores, J. A., & Sierro, F. J. (2014). The use of circularly polarized light for biometry, identification and estimation of mass of coccoliths. *Marine Micropaleontology*, *113*, 44–55. https://doi.org/10.1016/j.marmicro.2014.08.007

Hagino, K., Okada, H., & Matsuoka, H. (2005). Coccolithophore assemblages and morphotypes of *Emiliania huxleyi* in the boundary zone between the cold Oyashio and warm Kuroshio currents off the coast of Japan. *Marine Micropaleontology*, *55*(1–2), 19–47. https://doi.org/10.1016/j.marmicro.2005.02.002

Hammer-Muntz, O., Harper, D., & Ryan, P. (2001). *PAST: Paleontological statistics software package for education and data analysis. version 2.09*.

Hopkins, J., Henson, S. A., Painter, S. C., Tyrrell, T., & Poulton, A. J. (2015). Phenological characteristics of global coccolithophore blooms. *Global Biogeochemical Cycles*, *29*(2), 239–253. https://doi.org/10.1002/2014gb004919

Iglesias-Rodríguez, M. D., Brown, C. W., Doney, S. C., Kleypas, J., Kolber, D., Kolber, Z., et al. (2002). Representing key phytoplankton functional groups in ocean carbon cycle models: Coccolithophorids. *Global Biogeochemical Cycles*, *16*(4), 47-1–47-20

Jin, X., Liu, C., Poulton, A. J., Dai, M., & Guo, X. (2016). Coccolithophore responses to environmental variability in the South China sea: Species composition and calcite content. *Biogeosciences*, *13*(16), 4843–4861. https://doi.org/10.5194/bg-13-4843-2016

Jin, X., Liu, C., & Zhang, H. (2019). Coccolith morphological and assemblage responses to dissolution in the recent sediments of the East China Sea. *Marine Micropaleontology*, *152*, 101709. https://doi.org/10.1016/j.marmicro.2018.09.001

Jin, X. B., Liu, C. L., Zhao, Y. L., Zhang, Y. W., Wen, K., Lin, S., et al. (2019). Two production stages of coccolithophores in winter as revealed by sediment traps in the northern South China Sea. *Journal of Geophysical Research: Biogeosciences*, *124*(7), 2335–2350. https://doi.org/10.1029/2019jg005070

Liu, H., Yun, M., Zhang, X., Zhang, G., Thangaraj, S., Huang, K., & Sun, J. (2020). Biological calcification rate and species-specific contributions of coccolithophores to total calcite inventory in the eastern Indian ocean. *Journal of Geophysical Research: Biogeosciences*, *125*, e2019JG005547. https://doi.org/10.1029/2019jg005547

Marañón, E., Balch, W. M., Cermeño, P., González, N., Sobrino, C., Fernández, A., et al. (2016). Coccolithophore calcification is independent of carbonate chemistry in the tropical ocean. *Limnology & Oceanography*, *61*(4), 1345–1357.

Meier, K. J. S., Beaufort, L., Heussner, S., & Ziveri, P. (2014). The role of ocean acidification in *Emiliania huxleyi* coccolith thinning in the Mediterranean Sea. *Biogeosciences*, *11*(10), 2857–2869. https://doi.org/10.5194/bg-11-2857-2014

Meyer, J., & Riebesell, U. (2015). Reviews and syntheses: Responses of coccolithophores to ocean acidification: A meta-analysis. *Biogeosciences*, *12*(6), 1671–1682. https://doi.org/10.5194/bg-12-1671-2015

Nissen, C., Vogt, M., Münnich, M., Gruber, N., & Haumann, F. A. (2018). Factors controlling coccolithophore biogeography in the Southern Ocean. *Biogeosciences*, *15*(22), 6997–7024. https://doi.org/10.5194/bg-15-6997-2018

Paasche, E. (1973). Silicon and the ecology of marine plankton diatoms. II. Silicate-uptake kinetics in five diatom species. *Marine Biology*, *19*(3), 262–269. https://doi.org/10.1007/bf02097147

Patil, S. M., Mohan, R., Shetye, S. S., Vaz, V., Gazi, S., Choudhari, P. P., & Jafar, S. A. (2022). *Emiliania huxleyi* biometry and calcification response to the Indian sector of the Southern Ocean environmental gradients. *Palaeogeography, Palaeoclimatology, Palaeoecology*, *585*, 110725. https://doi.org/10.1016/j.palaeo.2021.110725

Pierrot, D. E., Lewis, E., & Wallace, D. W. R. (2006). *MS Excel program developed for CO2 system calculations. ORNL/CDIAC-105a, carbon dioxide information analysis Centre*. Oak Ridge National Laboratory, US Department of Energy

Poulton, A. J., Holligan, P. M., Charalampopoulou, A., & Adey, T. R. (2017). Coccolithophore ecology in the tropical and subtropical Atlantic ocean: New perspectives from the Atlantic Meridional transect (AMT) programme. *Progress in Oceanography*, *158*, 150–170. https://doi.org/10.1016/j.pocean.2017.01.003

Poulton, A. J., Painter, S. C., Young, J. R., Bates, N. R., Bowler, B., Drapeau, D., et al. (2013). The 2008 *Emiliania huxleyi* bloom along the Patagonian Shelf: Ecology, biogeochemistry, and cellular calcification. *Global Biogeochemical Cycles*, *27*(4), 1023–1033. https://doi.org/10.1002/2013gb004641

Poulton, A. J., Sanders, R., Holligan, P. M., Stinchcombe, M. C., Adey, T. R., Brown, L. A., & Chamberlain, K. (2006). Phytoplankton mineralization in the tropical and subtropical Atlantic Ocean. *Global Biogeochemical Cycles*, *20*(4). https://doi.org/10.1029/2006gb002712

Poulton, A. J., Young, J. R., Bates, N. R., & Balch, W. M. (2011). Biometry of detached *Emiliania huxleyi* coccoliths along the Patagonian shelf. *Marine Ecology Progress Series*, *443*, 1–17. https://doi.org/10.3354/meps09445

Priyadarshani, W. N. C., Ran, L., Wiesner, M. G., Chen, J., Ling, Z., Yu, S., & Ye, Y. (2019). Seasonal and interannual variability of coccolithophore flux in the northern South China Sea. *Deep Sea Research Part I: Oceanographic Research Papers*, *145*, 13–30. https://doi.org/10.1016/j.dsr.2019.01.004

Redfield, A. C., Ketchum, B. H., & Richards, F. A. (1963). The influence of organisms on the composition of sea-water. *The sea: Ideas and Observations on Progress in the Study of the Seas*, *2*, 26–77.

Saavedra-Pellitero, M., Baumann, K. H., Fuertes, M. Á., Schulz, H., Marcon, Y., Vollmar, N. M., et al. (2019). Calcification and latitudinal distribution of extant coccolithophores across the Drake Passage during late austral summer 2016. *Biogeosciences*, *16*(19), 3679–3702. https://doi.org/10.5194/bg-16-3679-2019

Saavedra-Pellitero, M., Baumann, K. H., Ullermann, J., & Lamy, F. (2017). Marine Isotope stage 11 in the Pacific sector of the Southern Ocean; a coccolithophore perspective. *Quaternary Science Reviews*, *158*, 1–14. https://doi.org/10.1016/j.quascirev.2016.12.020

Schlitzer, R. (2021). *Ocean data view*. Retrieved from https://odv.awi.de

Sun, J., An, B., Dai, M., & Li, T. (2011). Living coccolithophores in the Western south China sea in summer 2007. *Oceanologia et Limnologia Sinica*, *42*(2), 170–178.

Sun, J., Liu, H., Li, X., & Feng, Y. (2015). Distribution of living coccolithophores in the northern South China Sea in summer and winter. *Hai Yang Xue Bao*, *37*(12), 1–10.

Yang, T., & Wei, K. (2003). How many coccoliths are there in a coccosphere of the extant coccolithophorids? A compilation. *Journal of Nannoplankton Research*, *25*(1), 7–15.

Young, J. R., Geisen, M., Cros, L., Kleijne, A., Sprengel, C., Probert, I., & Østergaard, J. (2003). A guide to extant coccolithophore taxonomy. *Journal of Nannoplankton Research, Special Issue*, *1*, 1–132.

Young, J. R., Poulton, A. J., & Tyrrell, T. (2014). Morphology of *Emiliania huxleyi* coccoliths on the northwestern European shelf – Is there an influence of carbonate chemistry?*Biogeosciences*, *11*(17), 4771–4782. https://doi.org/10.5194/bg-11-4771-2014

Young, J. R., & Ziveri, P. (2000). Calculation of coccolith volume and its use in calibration of carbonate flux estimates. *Deep-Sea Research Part II Topical Studies in Oceanography*, *47*(9), 1679–1700. https://doi.org/10.1016/s0967-0645(00)00003-5

Ziveri, P., de Bernardi, B., Baumann, K. H., Stoll, H. M., & Mortyn, P. G. (2007). Sinking of coccolith carbonate and potential contribution to organic carbon ballasting in the deep ocean. *Deep Sea Research Part II: Topical Studies in Oceanography*, *54*(5–7), 659–675. https://doi.org/10.1016/j.dsr2.2007.01.006